

Physics/Astronomy 224 Spring 2012

Origin and Evolution of the Universe

Week 1

*Introduction:
GR, Distances, Surveys*

Joel Primack

University of California, Santa Cruz

Introduction

Modern cosmology – the study of the universe as a whole – is undergoing a scientific revolution. We can see back in time to the cosmic dark ages before galaxies formed and read the history of the early universe in the ripples of heat radiation still arriving from the Big Bang. We now know that everything that we can see makes up only about $\frac{1}{2}\%$ of the cosmic density, and that most of the universe is made of invisible stuff called “dark matter” and “dark energy.” The Λ CDM Dark Energy + Cold Dark Matter (“Double Dark”) theory based on this appears to be able to account for all the large scale features of the observable universe, including the heat radiation and the large scale distribution of galaxies, although there are possible problems understanding some details of the structure of galaxies.

Modern cosmology is developing humanity's first story of the origin and nature of the universe that might actually be true.

Modern Cosmology

A series of major discoveries has laid a lasting foundation for cosmology. Einstein's general relativity (1916) provided the conceptual foundation for the modern picture. Then Hubble discovered that "spiral nebulae" are large galaxies like our own Milky Way (1925), and that distant galaxies are receding from the Milky Way with a speed proportional to their distance (1929), which means that we live in an **expanding universe**. The discovery of the cosmic background radiation (1965) showed that the universe began in a very dense, hot, and homogeneous state: the Big Bang. This was confirmed by the discovery that the **cosmic background radiation** has exactly the same spectrum as heat radiation (1989), and the measured abundances of the light elements agree with the predictions of Big Bang theory if the **abundance of ordinary matter is about 4%** of critical density. Most of the matter in the universe is invisible particles which move very **sluggishly** in the early universe ("**Cold Dark Matter**"). Most of the energy density is mysterious **dark energy**.



Experimental and Historical Sciences

**both make predictions about new knowledge,
whether from experiments or from the past**

Historical Explanation Is Always Inferential

**Our age cannot look back to earlier things
Except where reasoning reveals their traces** Lucretius

Patterns of Explanation Are the Same in the Historical Sciences as in the Experimental Sciences

Specific conditions + General laws \Rightarrow Particular event

In history as anywhere else in empirical science, the explanation of a phenomenon consists in subsuming it under general empirical laws; and the criterion of its soundness is ... exclusively whether it rests on empirically well confirmed assumptions concerning initial conditions and general laws.

C.G. Hempel, Aspects of Scientific Explanation (1965), p. 240.

Successful Predictions of the Big Bang

First Prediction

First Confirmation

Expansion of the Universe

Friedmann 1922, Lemaitre 1927
based on Einstein 1916

Hubble 1929

Cosmic Background Radiation

Existence of CBR

Gamow, Alpher, Hermann 1948

Penzias & Wilson 1965

CBR Thermal Spectrum

Peebles 1966

COBE 1989

CBR Fluctuation Amplitude

Cold Dark Matter theory 1984

COBE 1992

CBR Acoustic Peak

BOOMERANG 2000

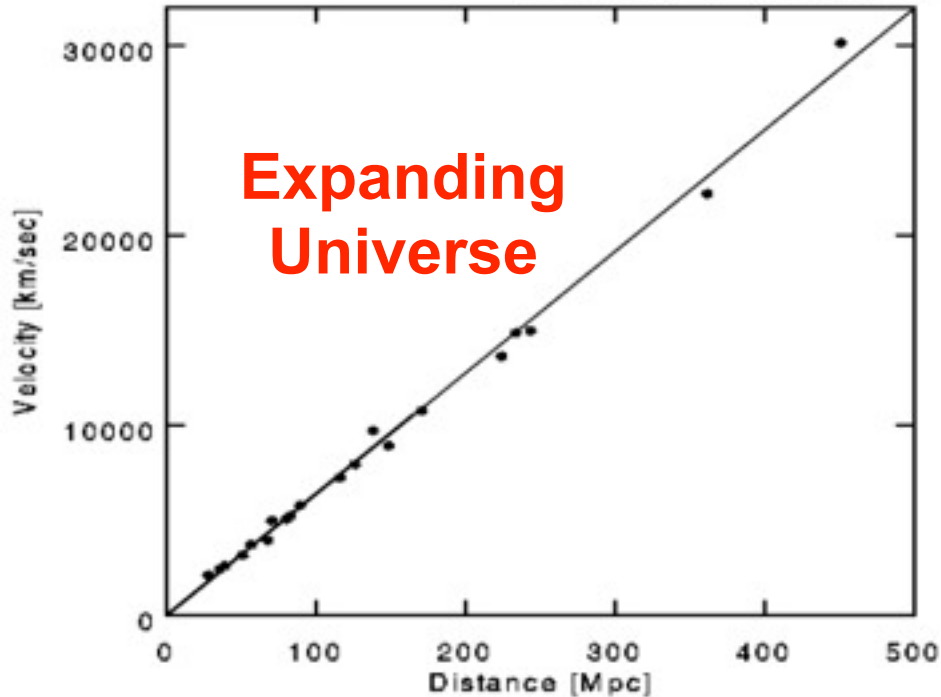
MAXIMA 2000

Light Element Abundances

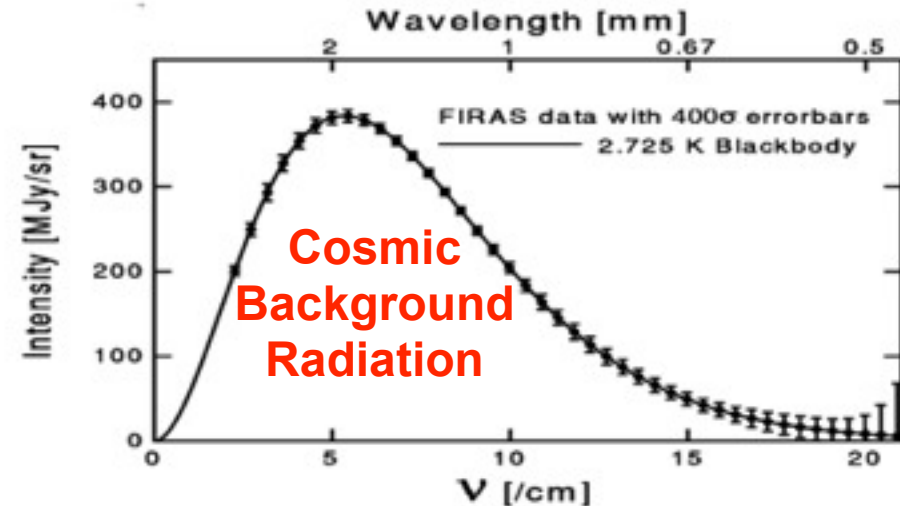
Peebles 1966, Wagoner 1967

D/H Tytler et al. 1997

Three Pillars of the Big Bang



A modern illustration of Hubble's Law, displaying the increase of recession speed of galaxies growing in direct proportion to their distance.

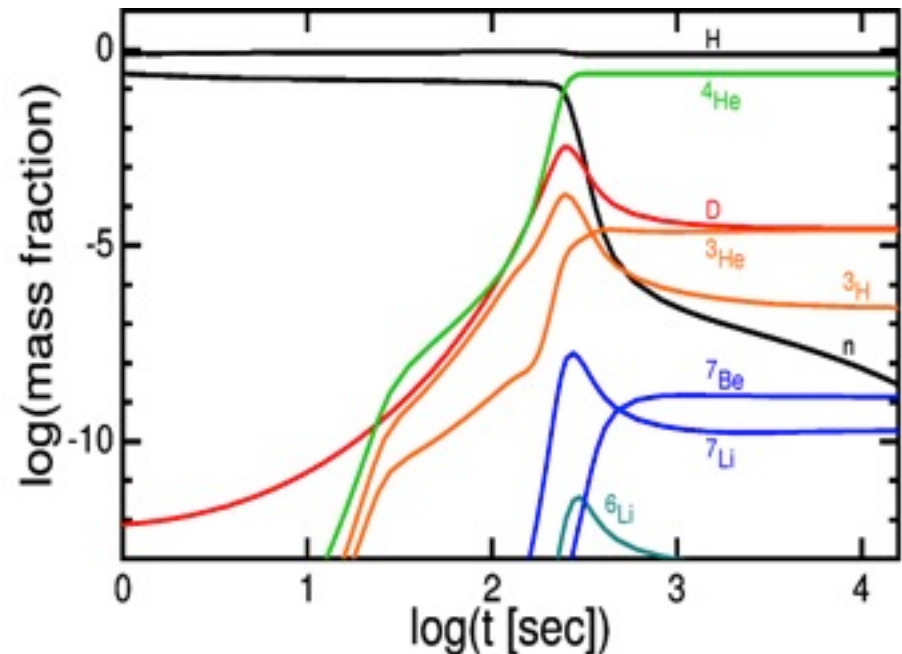


The variation of the intensity of the microwave background radiation with its frequency, as observed by the COBE satellite from above the Earth's atmosphere. The observations (boxes) display a perfect fit with the (solid) curve expected from pure heat radiation with a temperature of 2.73°K.

Big Bang Nucleosynthesis

The detailed production of the lightest elements out of protons and neutrons during the first three minutes of the universe's history. The nuclear reactions occur rapidly when the temperature falls below a billion degrees Kelvin. Subsequently, the reactions are shut down, because of the rapidly falling temperature and density of matter in the expanding universe.

Caution: ${}^7\text{Li}$ may now be discordant



Dynamical effects of the cosmological constant

Ofer Lahav,¹ Per B. Lilje,² Joel R. Primack³ and Martin J. Rees¹

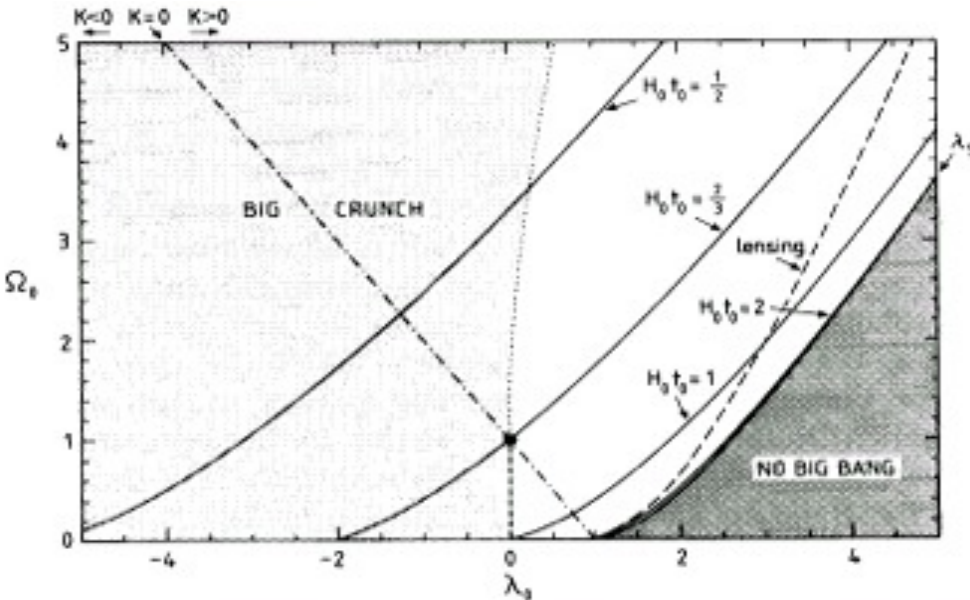
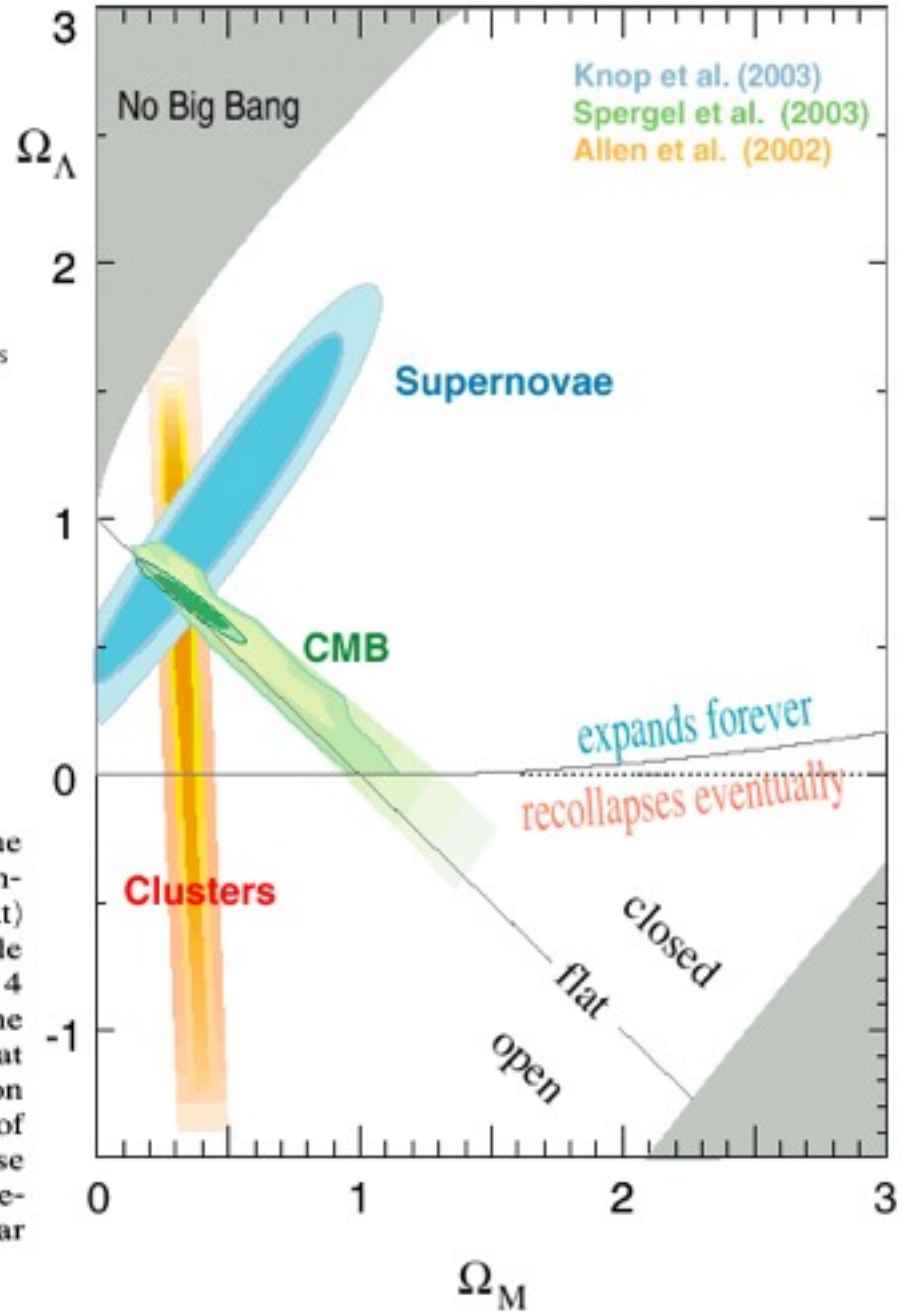


Figure 1. The phase-space of the density parameter Ω_0 and the cosmological constant $\lambda_0 \equiv \Lambda / (3 H_0^2)$ with various fundamental constraints. The dashed-dotted line indicates an inflationary (i.e. flat) universe. Note that some open models will have a Big Crunch, while some closed models will expand forever. The solid lines show 4 values for the age of the universe $H_0 t_0$, and the dashed line is the constraint of Gott *et al.* (1989) from a normally lensed quasar at $z = 3.27$. The boundary (λ_s) of the shaded 'No Big Bang' region corresponds to a coasting phase in the past, while the boundary of the 'Big Crunch' (for $\Omega_0 > 1$) region corresponds to a coasting phase in the future. We see that the permitted range in the $(\lambda_0 - \Omega_0)$ phase-space is fairly small, but allows values different from the popular point ($\Omega_0 = 1, \lambda_0 = 0$).

Supernova Cosmology Project



General Relativity and Cosmology

GR: MATTER TELLS SPACE
HOW TO CURVE

CURVED SPACE TELLS
MATTER HOW TO MOVE

$$R^{\mu\nu} - \frac{1}{2}Rg^{\mu\nu} = 8\pi GT^{\mu\nu} + \Lambda g^{\mu\nu}$$

$$\frac{du^\mu}{ds} + \Gamma^\mu_{\alpha\beta} u^\alpha u^\beta = 0$$

Cosmological Principle: on large scales, space is uniform and isotropic. COBE-Copernicus Theorem: If all observers observe a nearly-isotropic Cosmic Background Radiation (CBR), then the universe is locally nearly homogeneous and isotropic – i.e., is approximately described by the Friedmann-Robertson-Walker metric

$$ds^2 = dt^2 - a^2(t) [dr^2 (1 - kr^2)^{-1} + r^2 d\Omega^2]$$

with curvature constant $k = -1, 0, \text{ or } +1$. Substituting this metric into the Einstein equation at left above, we get the Friedmann eq.

Friedmann-Robertson-Walker Framework (homogeneous, isotropic universe)

FRW E(00) $\frac{\dot{a}^2}{a^2} = \frac{8\pi}{3}G\rho - \frac{k}{a^2} + \frac{\Lambda}{3}$ ← Friedmann equation

FRW E(ii) $\frac{2\ddot{a}}{a} + \frac{\dot{a}^2}{a^2} = -8\pi Gp - \frac{k}{a^2} + \Lambda$

$$H_0 \equiv 100h \text{ km s}^{-1} \text{ Mpc}^{-1}$$

$$\equiv 70h_{70} \text{ km s}^{-1} \text{ Mpc}^{-1}$$

$$\frac{E(00)}{H_0^2} \Rightarrow 1 = \Omega_0 - \frac{k}{H_0^2} + \Omega_\Lambda \text{ with } H \equiv \frac{\dot{a}}{a}, a_0 \equiv 1, \Omega_0 \equiv \frac{\rho_0}{\rho_c}, \Omega_\Lambda \equiv \frac{\Lambda}{3H_0^2},$$

$$\rho_{c,0} \equiv \frac{3H_0^2}{8\pi G} = 1.36 \times 10^{11} h_{70}^2 M_\odot \text{ Mpc}^{-3}$$

$$E(ii) - E(00) \Rightarrow \frac{2\ddot{a}}{a} = -\frac{8\pi}{3}G\rho - 8\pi Gp + \frac{2}{3}\Lambda$$

$$\text{Divide by } 2E(00) \Rightarrow q_0 \equiv -\left(\frac{\ddot{a}}{a} \frac{a^2}{\dot{a}^2}\right)_0 = \frac{\Omega_0}{2} - \Omega_\Lambda$$

$$E(00) \Rightarrow t_0 = \int_0^1 \frac{da}{a} \left[\frac{8\pi}{3}G\rho - \frac{k}{a^2} + \frac{\Lambda}{3} \right]^{-\frac{1}{2}} = H_0^{-1} \int_0^1 \frac{da}{a} \left[\frac{\Omega_0}{a^3} - \frac{k}{H_0^2 a^2} + \Omega_\Lambda \right]^{-\frac{1}{2}}$$

$$t_0 = H_0^{-1} f(\Omega_0, \Omega_\Lambda) \quad H_0^{-1} = 9.78 h^{-1} \text{ Gyr} \quad f(1, 0) = \frac{2}{3}$$

$$= 13.97 h_{70}^{-1} \text{ Gyr} \quad f(0, 0) = 1$$

$$f(0, 1) = \infty$$

$$f(0.3, 0.7) = 0.964$$

$$[E(00)a^3]' \text{ vs. } E(ii) \Rightarrow \frac{\partial}{\partial a}(\rho a^3) = -3p a^2 \text{ ("continuity")}$$

Given eq. of state $p = p(\rho)$, integrate to determine $\rho(a)$,
integrate E(00) to determine $a(t)$

Matter: $p = 0 \Rightarrow \rho = \rho_0 a^{-3}$ (assumed above in q_0, t_0 eqs.)

Radiation: $p = \frac{\rho}{3}, k = 0 \Rightarrow \rho \propto a^{-4}$

Measuring Distances in the Universe

Primary Distance Indicators

Trigonometric parallax

α Centauri 1.35 pc - first measured by Thomas Henderson 1832

61 Cygni 3.48 pc - by Friedrich Wilhelm Bessel in 1838

Only a few stars to < 30 pc, until the Hipparcos satellite 1997 measured distances of 118,000 stars to about 100 pc, about 20,000 stars to $< 10\%$.

Proper motions

Moving cluster method

Mainly for the Hyades, at about 100 pc. Now supplanted by Hipparcos.

Distance to Cepheid ζ Geminorum = 336 ± 44 pc

Using Doppler to measure change of diameter, and interferometry to measure change of angular diameter.

Similar methods for Type II SN, for stars in orbit about the Sagittarius A* SMBH (gives distance 8.0 ± 0.4 kpc to Galactic Center), for radio maser in NGC 4258 (7.2 ± 0.5 Mpc), etc.

Apparent Luminosity of various types of stars

$L = 10^{-2M/5} 3.02 \times 10^{35} \text{ erg sec}^{-1}$ where $M_{\text{vis}} = + 4.82$ for the sun

Apparent luminosity $\ell = L (4\pi d^2)^{-1}$ for nearby objects,
related to apparent magnitude m by $\ell = 10^{-2m/5} (2.52 \times 10^{-5} \text{ erg cm}^{-2} \text{ s}^{-1})$

Distance modulus $m - M$ related to distance by $d = 10^{1 + (m - M)/5} \text{ pc}$

Main sequence stars were calibrated by Hipparchos distances and the Hubble Space Telescope Fine Guidance Sensor

Red clump (He burning) stars.

RR Lyrae Stars - variables with periods 0.2 - 0.8 days

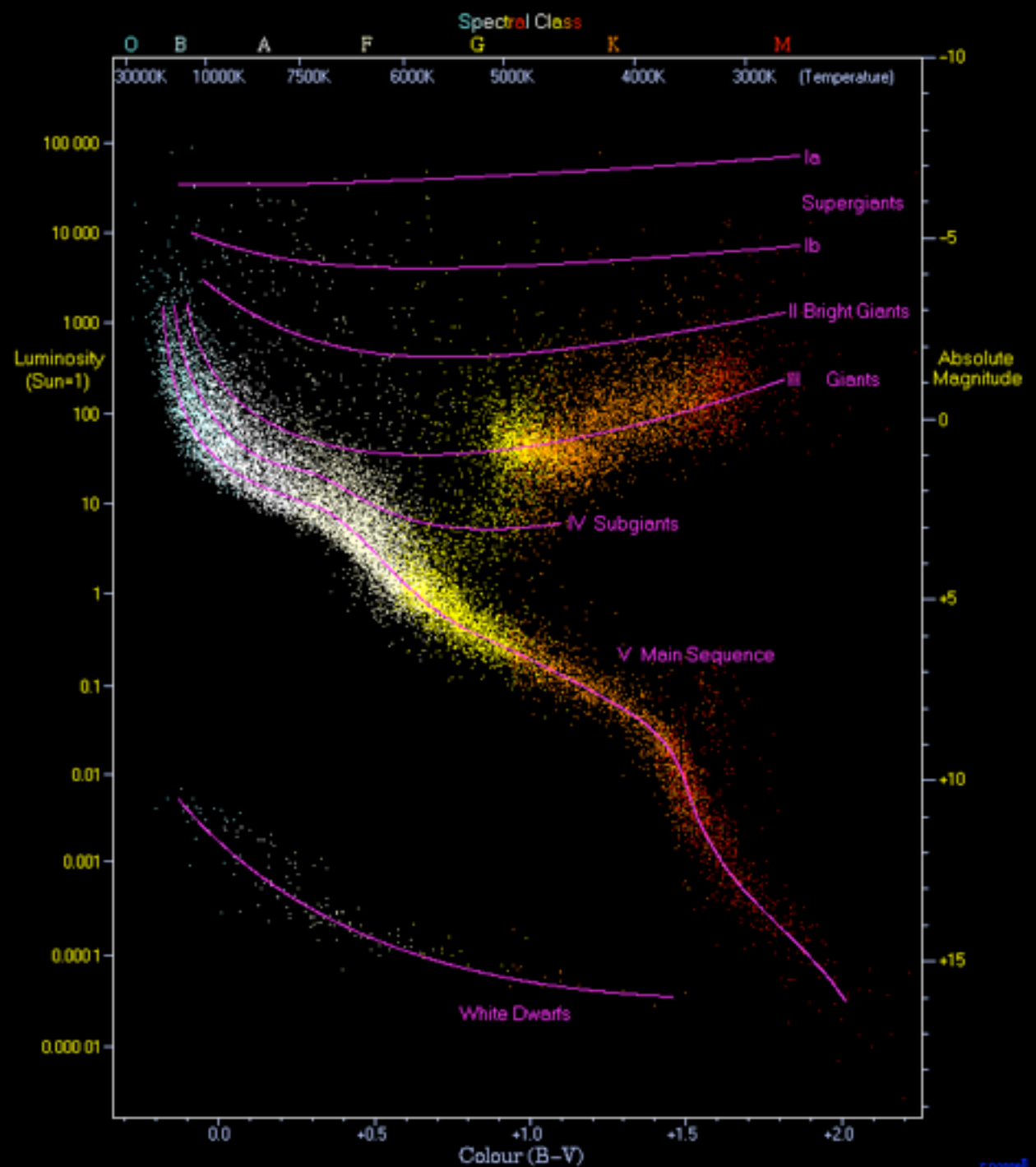
Eclipsing binaries - v from Doppler, ellipticity from $v(t)$, radius of primary from duration of eclipse, T from spectrum, gives $L = \sigma T^4 \pi R^2$

Cepheid variables - bright variable stars with periods 2 - 45 days

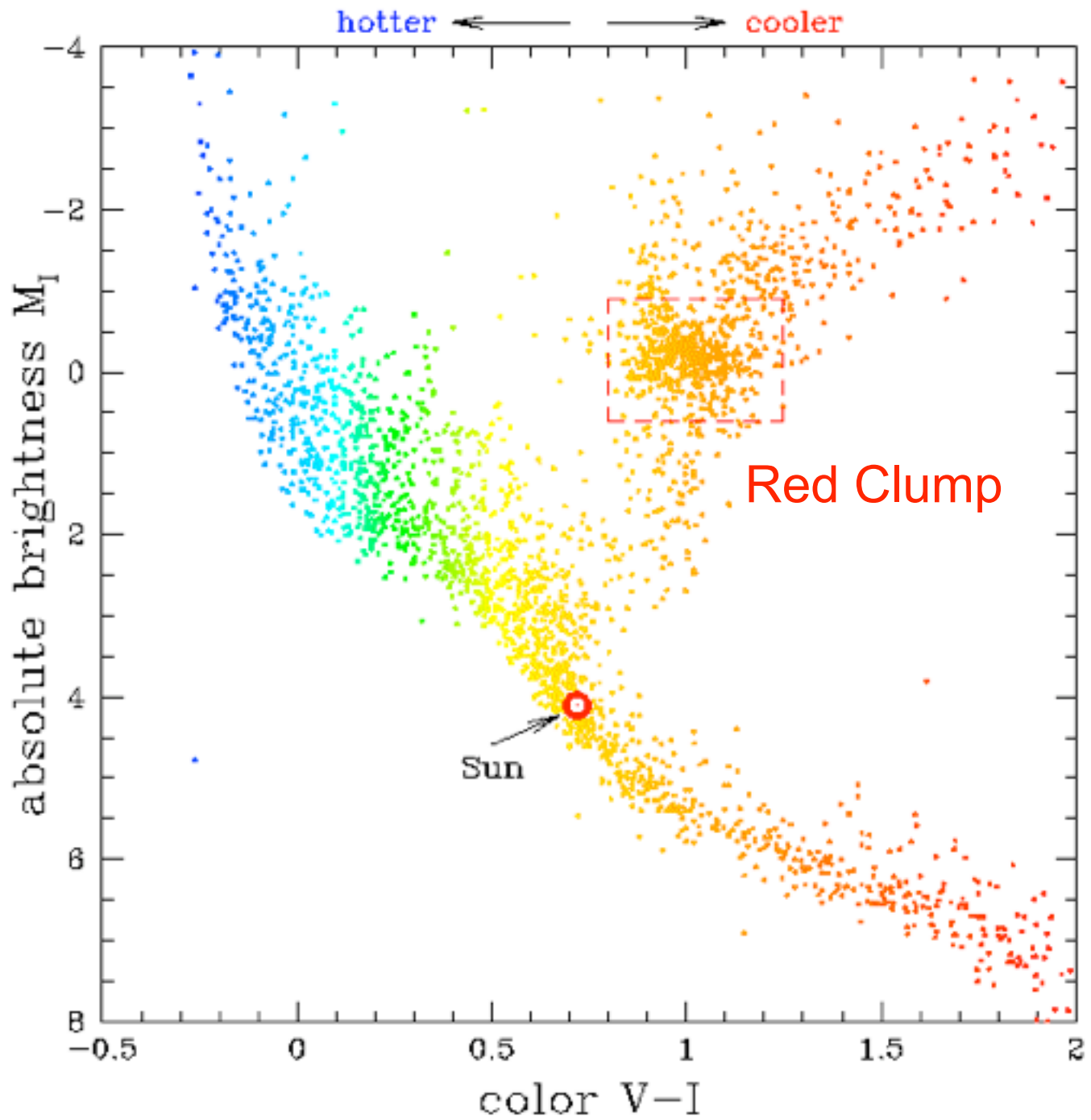


Henrietta Swan Leavitt in 1912 discovered the Cepheid period-luminosity relation in the SMC, now derived mainly from the LMC. This was the basis for Hubble's 1923 finding that M32 is far outside the Milky Way. Best value today for the LMC distance modulus $m - M = 18.50$ (see Weinberg, *Cosmology*, p. 25), or $d_{\text{LMC}} = 50.1 \text{ kpc}$.

Hertzprung-Russell Diagram



Hertzprung-Russell Diagram



Secondary Distance Indicators

Tully-Fisher relation

Faber-Jackson relation

Fundamental plane

Type Ia supernovae

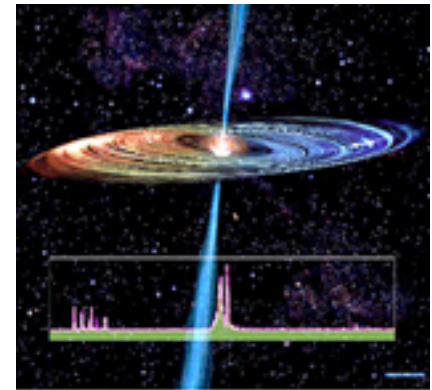
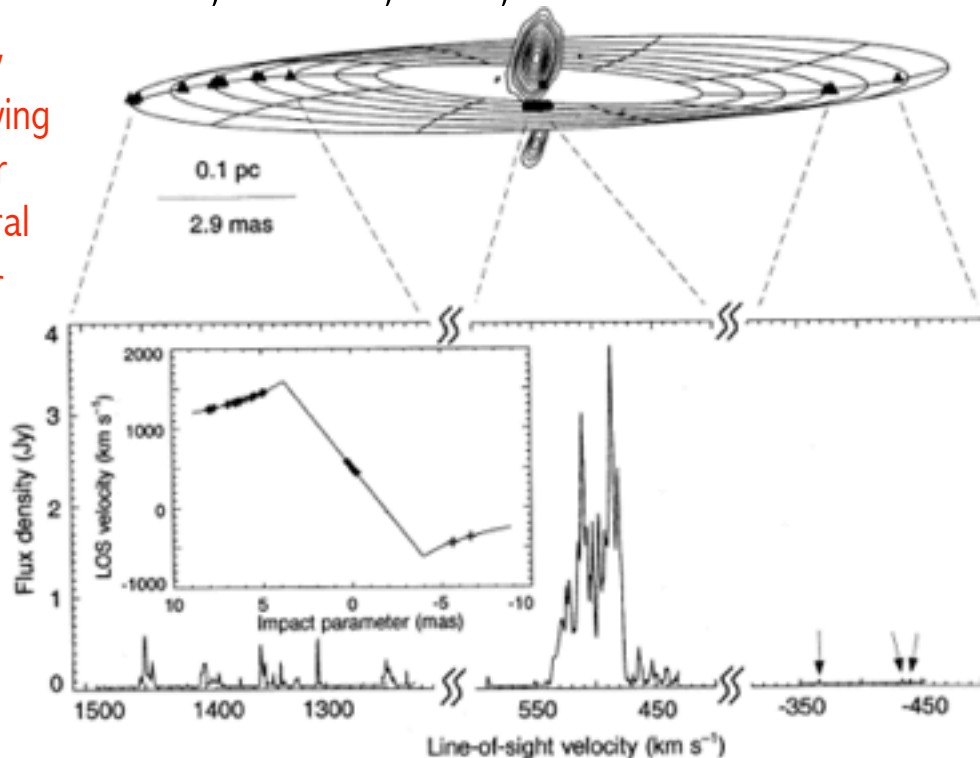
Surface brightness fluctuations

Extragalactic water masers

Extragalactic water masers

A geometric distance to the galaxy NGC4258 from orbital motions in a nuclear gas disk
J. R. Herrnstein et al. 1999, Nature, 400, 539. Dist to NGC4258 = 7.2 ± 0.3 Mpc.

The distance is found by measuring the time-varying Doppler shift and proper motion around the central black hole. The Doppler shift is maximum when an object is moving along the l.o.s. and the proper motion is maximum when the object is moving perpendicular to the l.o.s.



Artist's Conception

$$M_{\text{BH}} = 3.9 \pm 0.1 M_{\text{sun}}$$

Figure 1 The NGC4258 water maser. The upper panel shows the best-fitting warped-disk model superposed on actual maser positions as measured by the VLBA of the NRAO, with top as North. The filled square marks the centre of the disk, as determined from a global disk-fitting analysis⁸. The filled triangles show the positions of the high-velocity masers, so called because they occur at frequencies corresponding to Doppler shifts of $\sim \pm 1,000 \text{ km s}^{-1}$ with respect to the galaxy systemic velocity of $\sim 470 \text{ km s}^{-1}$. This is apparent in the VLBA total power spectrum (lower panel). The inset shows line-of-sight (LOS) velocity versus impact parameter for the best-fitting keplerian disk, with the maser data superposed. The high-velocity masers trace a keplerian curve to better than 1%. Monitoring of these features indicates that they drift by less than $\sim 1 \text{ km s}^{-1} \text{ yr}^{-1}$ (refs 14–16) and requires that they lie within $5\text{--}10^\circ$ of the midline, the intersection of the disk with the plane of the sky. The LOS velocities of the systemic masers are

centred about the systemic velocity of the galaxy. The positions (filled circles in upper panel) and LOS velocities of these masers imply that they subtend $\sim 8^\circ$ of disk azimuth centred about the LOS to the central mass, and the observed acceleration ($8\text{--}10 \text{ km s}^{-1} \text{ yr}^{-1}$) of these features^{14,15} unambiguously places them along the near edge of the disk. The approximately linear relationship between systemic maser impact parameter and LOS velocity demonstrates that the disk is very thin¹⁷ (aspect ratio $\ll 0.2\%$) and that these masers are confined to a narrow annulus in the disk. The magnitude of the velocity gradient (Ω_{a}) implies a mean systemic radius, (r_{a}), of 3.9 mas which, together with the positions of the high-velocity masers, constrains the disk inclination, i_{a} , to be $\sim 82 \pm 1^\circ$ (90° for edge-on). Finally, VLBA continuum images^{7,9} are included as contours in the upper panel. The 22-GHz radio emission traces a sub-parsec-scale jet elongated along the rotation axis of the disk and well-aligned with a luminous, kiloparsec-scale jet¹⁸.

Extragalactic water masers

A geometric distance to the galaxy NGC4258 from orbital motions in a nuclear gas disk
J. R. Herrnstein et al. 1999, Nature, 400, 539. Dist to NGC4258 = 7.2 ± 0.3 Mpc.

we conclude that $\langle \dot{v}_{\text{LOS}} \rangle = 9.3 \pm 0.3 \text{ km s}^{-1} \text{ yr}^{-1}$ and $\langle \dot{\theta}_x \rangle = 31.5 \pm 1 \mu\text{as yr}^{-1}$, where these (and all subsequent) uncertainties are 1σ values.

To convert the maser proper motions and accelerations into a geometric distance, we express $\langle \dot{\theta}_x \rangle$ and $\langle \dot{v}_{\text{LOS}} \rangle$ in terms of the distance and four disk parameters:

$$\langle \dot{\theta}_x \rangle = 31.5 \left[\frac{D_6}{7.2} \right]^{-1} \left[\frac{\Omega_s}{282} \right]^{1/3} \left[\frac{M_{7.2}}{3.9} \right]^{1/3} \left[\frac{\sin i_s}{\sin 82.3^\circ} \right]^{-1} \left[\frac{\cos \alpha_s}{\cos 80^\circ} \right] \mu\text{as yr}^{-1} \quad (1)$$

and

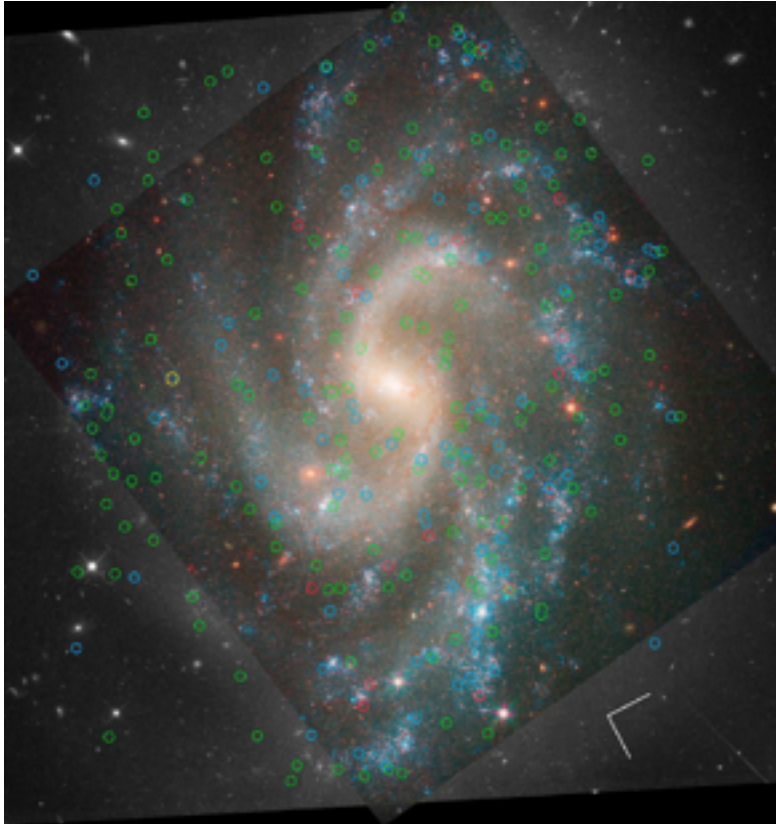
$$\langle \dot{v}_{\text{LOS}} \rangle = 9.2 \left[\frac{D_6}{7.2} \right]^{-1} \left[\frac{\Omega_s}{282} \right]^{4/3} \left[\frac{M_{7.2}}{3.9} \right]^{1/3} \left[\frac{\sin i_s}{\sin 82.3^\circ} \right]^{-1} \text{ km s}^{-1} \text{ yr}^{-1} \quad (2)$$

Here D_6 is the distance in Mpc, α_s is the disk position angle (East of North) at $\langle r_s \rangle$, and $M_{7.2}$ is $M/D \sin^2 i_s$ as derived from the high-velocity rotation curve and evaluated at $D = 7.2$ Mpc and $i_s = 82.3^\circ$ (in units of $10^7 M_\odot$). $\Omega_s \equiv (GM_{7.2}/\langle r_s \rangle^3)^{1/2}$ is the projected disk angular velocity at $\langle r_s \rangle$

Determining the Hubble constant H_0 using multiple calibrators

A 3% SOLUTION: DETERMINATION OF THE HUBBLE CONSTANT WITH THE *HUBBLE SPACE TELESCOPE* AND WIDE FIELD CAMERA 3*

Adam G. Riess et al. THE ASTROPHYSICAL JOURNAL, 730:119 (18pp), 2011 April 1



HST images of NGC 5584 and NGC 4038/9.. The positions of Cepheids with periods in the range $P > 60$ days, $30 \text{ days} < P < 60 \text{ days}$, and $10 \text{ days} < P < 30 \text{ days}$ are indicated by red, blue, and green circles, respectively. A yellow circle indicates the position of the host galaxy's SN Ia. The orientation is indicated by the compass rose whose vectors have lengths of 15'' and indicate north and east. The black and white regions of the images show the WFC3 optical data and the color includes the WFC3-IR data.

Determining the Hubble constant H_0 using multiple calibrators

A 3% SOLUTION: DETERMINATION OF THE HUBBLE CONSTANT WITH THE *HUBBLE SPACE TELESCOPE* AND WIDE FIELD CAMERA 3*

Adam G. Riess et al. THE ASTROPHYSICAL JOURNAL, 730:119 (18pp), 2011 April 1

$H_0 = 73.8 \pm 2.4 \text{ km s}^{-1} \text{ Mpc}^{-1}$ including systematic errors, corresponding to a 3.3% uncertainty.

Figure 9. Uncertainties in the determination of the Hubble constant. Uncertainties are squared to show their contribution to the quadrature sum. These terms are given in Table 5.

Table 5
 H_0 Error Budget for Cepheid and SN Ia Distance Ladders^a

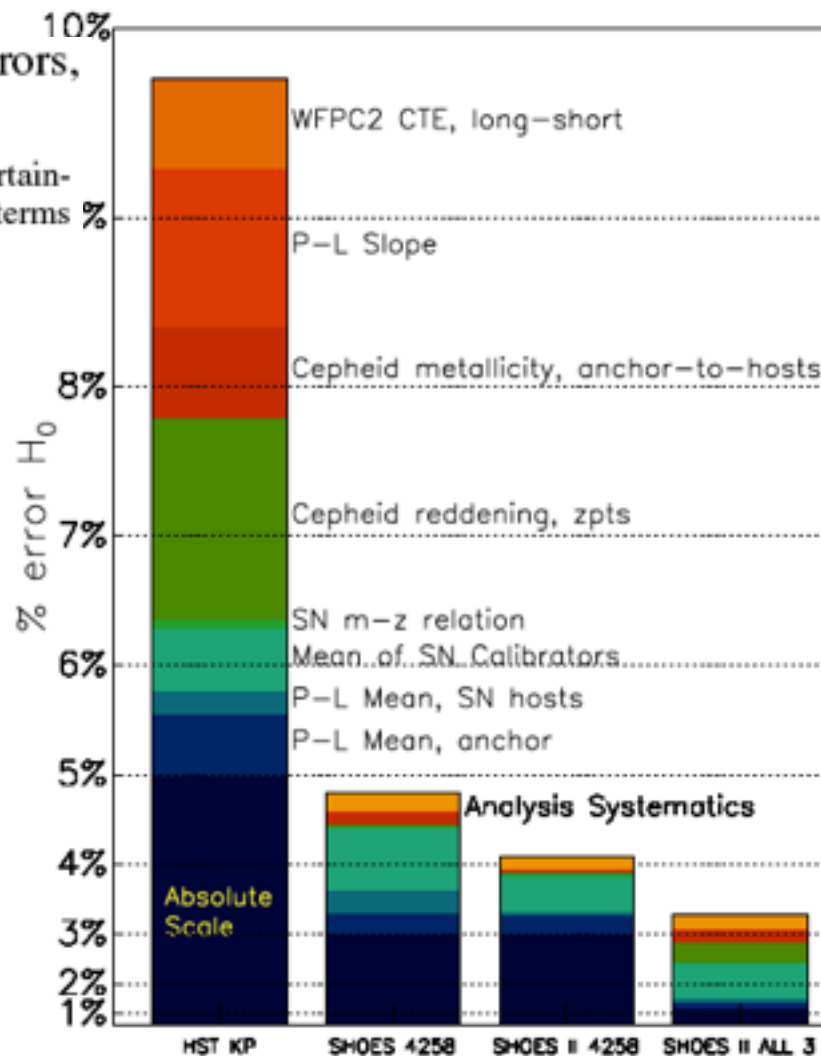
Term	Description	Previous LMC	R09 N4258	Here N4258	Here All Three ^b
σ_{anchor}	Anchor distance	5%	3%	3%	1.3%
$\sigma_{\text{anchor-PL}}$	Mean of $P-L$ in anchor	2.5%	1.5%	1.4%	0.7% ^c
$\sigma_{\text{host-PL}/\sqrt{n}}$	Mean of $P-L$ values in SN hosts	1.5%	1.5%	0.6%	0.6%
$\sigma_{\text{SN}/\sqrt{n}}$	Mean of SN Ia calibrators	2.5%	2.5%	1.9%	1.9%
σ_{m-z}	SN Ia $m-z$ relation	1%	0.5%	0.5%	0.5%
$R\sigma_{\lambda,1,2}$	Cepheid reddening, zero points, anchor-to-hosts	4.5%	0.3%	0.0%	1.4%
σ_Z	Cepheid metallicity, anchor-to-hosts	3%	1.1%	0.6%	1.0%
σ_{PL}	$P-L$ slope, $\Delta \log P$, anchor-to-hosts	4%	0.5%	0.4%	0.6%
σ_{WFPC2}	WFPC2 CTE, long-short	3%	0%	0%	0%
Subtotal, σ_{H_0}		10%	4.7%	4.0%	2.9%
Analysis systematics		NA	1.3%	1.0%	1.0%
Total, σ_{H_0}		10%	4.8%	4.1%	3.1%

Notes.

^a Derived from diagonal elements of the covariance matrix propagated via the error matrices associated with Equations (1), (3), (7), and (8).

^b Using the combination of all three calibrations of the Cepheid distance scale, LMC, MW parallaxes, and NGC 4258.

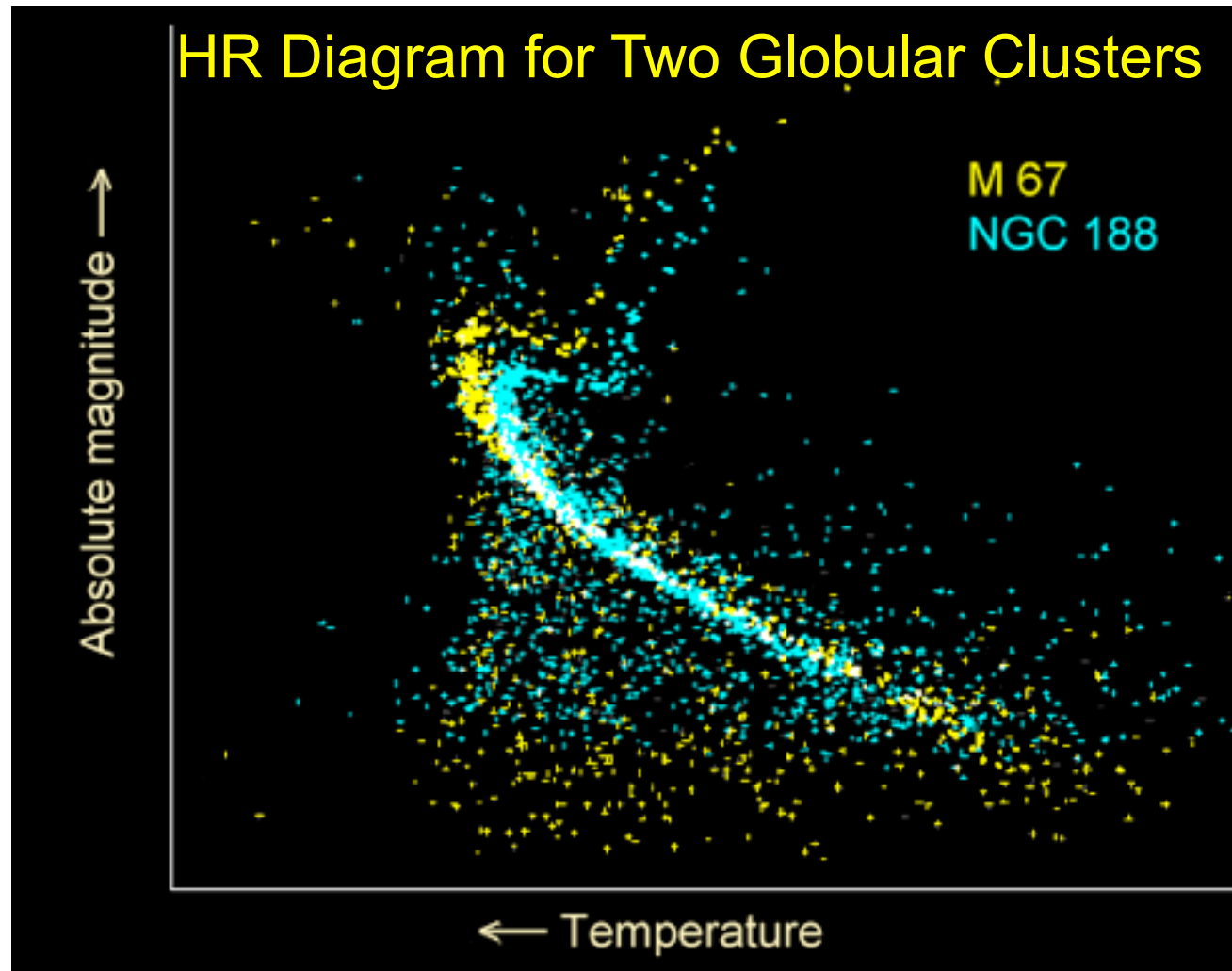
^c For MW parallax, this term is already included with the term above.



The Age of the Universe

In the mid-1990s there was a crisis in cosmology, because the age of the old Globular Cluster stars in the Milky Way, then estimated to be 16 ± 3 Gyr, was higher than the expansion age of the universe, which for a critical density ($\Omega_m = 1$) universe is 9 ± 2 Gyr (with the Hubble parameter $h = 0.72 \pm 0.07$).

But when the data from the Hipparcos astrometric satellite became available in 1997, it showed that the distance to the Globular Clusters had been underestimated, which implied that their ages are 12 ± 3 Gyr.



The Age of the Universe

In the mid-1990s there was a crisis in cosmology, because the age of the old Globular Cluster stars in the Milky Way, then estimated to be 16 ± 3 Gyr, was higher than the expansion age of the universe, which for a critical density ($\Omega_m = 1$) universe is 9 ± 2 Gyr (with the Hubble parameter $h = 0.72 \pm 0.07$). But when the data from the Hipparcos astrometric satellite became available in 1997, it showed that the distance to the Globular Clusters had been underestimated, which implied that their ages are 12 ± 3 Gyr.

Several lines of evidence now show that the universe does not have $\Omega_m = 1$ but rather $\Omega_{\text{tot}} = \Omega_m + \Omega_\Lambda = 1.0$ with $\Omega_m \approx 0.3$, which gives an expansion age of about 14 Gyr.

Moreover, a new type of age measurement based on radioactive decay of Thorium-232 (half-life 14.1 Gyr) measured in a number of stars gives a completely independent age of 14 ± 3 Gyr. A similar measurement, based on the first detection in a star of Uranium-238 (half-life 4.47 Gyr), gives 12.5 ± 3 Gyr.

All the recent measurements of the age of the universe are thus in excellent agreement. It is reassuring that three completely different clocks – stellar evolution, expansion of the universe, and radioactive decay – agree so well.

General Relativity

GR follows from the principle of equivalence and Einstein's equation $G_{\mu\nu} \equiv R_{\mu\nu} - \frac{1}{2}Rg_{\mu\nu} = -8\pi GT_{\mu\nu}$.* Einstein had intuited the local equivalence of gravity and acceleration in 1907 (Pais, p. 179), but it was not until November 1915 that he developed the final form of the GR equation.

(Gravitation & Cosmology)

It can be derived from the following assumptions (Weinberg, p. 153):

1. The l.h.s. $G_{\mu\nu}$ is a tensor
2. $G_{\mu\nu}$ consists only of terms linear in second derivatives or quadratic in first derivatives of the metric tensor $g_{\mu\nu}$ ($\Leftrightarrow G_{\mu\nu}$ has dimension L^{-2})
3. Since $T_{\mu\nu}$ is symmetric in $\mu\nu$, so is $G_{\mu\nu}$
4. Since $T_{\mu\nu}$ is conserved (covariant derivative $T^{\mu}_{\nu;\mu}=0$) so also $G^{\mu}_{\nu;\mu}=0$
5. In the weak field limit where $g_{00} \approx -(1+2\phi)$, satisfying the Poisson equation $\nabla^2\phi=4\pi G\rho$ (i.e., $\nabla^2g_{00}=-8\pi GT_{00}$), we must have $G_{00}=\nabla^2g_{00}$

*Note: we're here using the metric $-1, 1, 1, 1$ as in Dodelson, Weinberg.

Einstein's equation can also be derived from an action principle, varying the total action $I = I_M + I_G$, where I_M is the action of matter and I_G is that of gravity:

$$I_G = - \frac{1}{16\pi G} \int R(x) \sqrt{g(x)} d^4x$$

(see, e.g., Weinberg, p. 364). The curvature scalar $R \equiv R_{\mu\nu} g^{\mu\nu}$ is the obvious term to insert in I_G since a scalar connected with the metric is needed and it is the only one, unless higher powers R^2 , R^3 or higher derivatives $\square R$ are used, which will lead to higher-order or higher-derivative terms in the gravity equation.

Einstein realized in 1916 that the 5th postulate above isn't strictly necessary – merely that the equation reduce to the Newtonian Poisson equation within observational errors, which allows the inclusion of a small cosmological constant term. In the action derivation, such a term arises if we just add a constant to R .

One elementary equivalence principle is the kind Newton had in mind when he stated that the property of a body called “mass” is proportional to the “weight”, and is known as the weak equivalence principle (WEP). An alternative statement of WEP is that the trajectory of a freely falling “test” body (one not acted upon by such forces as electromagnetism and too small to be affected by tidal gravitational forces) is independent of its internal structure and composition. In the simplest case of dropping two different bodies in a gravitational field, WEP states that the bodies fall with the same acceleration (this is often termed the Universality of Free Fall, or UFF).

The Einstein equivalence principle (EEP) is a more powerful and far-reaching concept; it states that:

1. WEP is valid.
2. The outcome of any local non-gravitational experiment is independent of the velocity of the freely-falling reference frame in which it is performed.
3. The outcome of any local non-gravitational experiment is independent of where and when in the universe it is performed.

The second piece of EEP is called local Lorentz invariance (LLI), and the third piece is called local position invariance (LPI).

For example, a measurement of the electric force between two charged bodies is a local non-gravitational experiment; a measurement of the gravitational force between two bodies (Cavendish experiment) is not.

The Einstein equivalence principle is the heart and soul of gravitational theory, for it is possible to argue convincingly that if EEP is valid, then gravitation must be a “curved spacetime” phenomenon, in other words, the effects of gravity must be equivalent to the effects of living in a curved spacetime. As a consequence of this argument, the only theories of gravity that can fully embody EEP are those that satisfy the postulates of “metric theories of gravity”, which are:

1. Spacetime is endowed with a symmetric metric.
2. The trajectories of freely falling test bodies are geodesics of that metric.
3. In local freely falling reference frames, the non-gravitational laws of physics are those written in the language of special relativity.

Friedmann- Robertson- Walker Framework (homogeneous, isotropic universe)

$$\text{FRW } E(00) \quad \frac{\dot{a}^2}{a^2} = \frac{8\pi}{3}G\rho - \frac{k}{a^2} + \frac{\Lambda}{3} \quad \leftarrow \text{Friedmann equation}$$

$$\text{FRW } E(ii) \quad \frac{2\ddot{a}}{a} + \frac{\dot{a}^2}{a^2} = -8\pi Gp - \frac{k}{a^2} + \Lambda$$

$$H_0 \equiv 100h \text{ km s}^{-1} \text{ Mpc}^{-1} \\ \equiv 70h_{70} \text{ km s}^{-1} \text{ Mpc}^{-1}$$

$$\frac{E(00)}{H_0^2} \Rightarrow 1 = \Omega_0 - \frac{k}{H_0^2} + \Omega_\Lambda \text{ with } H \equiv \frac{\dot{a}}{a}, a_0 \equiv 1, \Omega_0 \equiv \frac{\rho_0}{\rho_c}, \Omega_\Lambda \equiv \frac{\Lambda}{3H_0^2}, \\ \rho_{c,0} \equiv \frac{3H_0^2}{8\pi G} = 1.36 \times 10^{11} h_{70}^2 M_\odot \text{ Mpc}^{-3}$$

$$E(ii) - E(00) \Rightarrow \frac{2\ddot{a}}{a} = -\frac{8\pi}{3}G\rho - 8\pi Gp + \frac{2}{3}\Lambda$$

$$\text{Divide by } 2E(00) \Rightarrow q_0 \equiv -\left(\frac{\ddot{a}}{a} \frac{a^2}{\dot{a}^2}\right)_0 = \frac{\Omega_0}{2} - \Omega_\Lambda$$

$$E(00) \Rightarrow t_0 = \int_0^1 \frac{da}{a} \left[\frac{8\pi}{3}G\rho - \frac{k}{a^2} + \frac{\Lambda}{3} \right]^{-\frac{1}{2}} = H_0^{-1} \int_0^1 \frac{da}{a} \left[\frac{\Omega_0}{a^3} - \frac{k}{H_0^2 a^2} + \Omega_\Lambda \right]^{-\frac{1}{2}}$$

$$t_0 = H_0^{-1} f(\Omega_0, \Omega_\Lambda) \quad H_0^{-1} = 9.78 h^{-1} \text{ Gyr} \quad f(1, 0) = \frac{2}{3} \\ = 13.97 h_{70}^{-1} \text{ Gyr} \quad f(0, 0) = 1 \\ f(0, 1) = \infty \\ f(0.3, 0.7) = 0.964$$

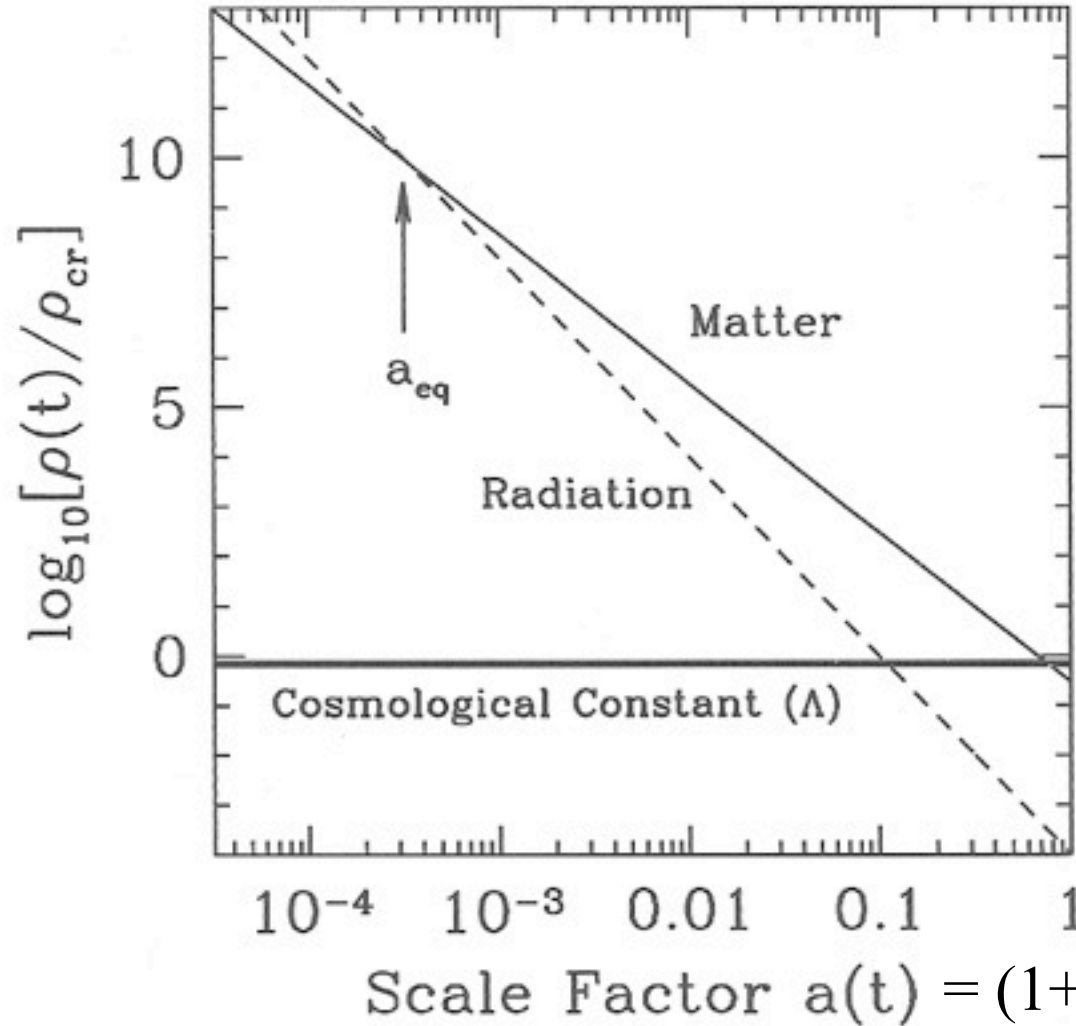
$$[E(00)a^3]' \text{ vs. } E(ii) \Rightarrow \frac{\partial}{\partial a}(\rho a^3) = -3p a^2 \text{ ("continuity")}$$

Given eq. of state $p = p(\rho)$, integrate to determine $\rho(a)$,
integrate $E(00)$ to determine $a(t)$

$$\text{Matter: } p = 0 \Rightarrow \rho = \rho_0 a^{-3} \text{ (assumed above in } q_0, t_0 \text{ eqs.)}$$

$$\text{Radiation: } p = \frac{\rho}{3}, k = 0 \Rightarrow \rho \propto a^{-4}$$

Evolution of Densities of Radiation, Matter, & Λ



$z = \text{redshift}$

Figure 1.3. Energy density vs scale factor for different constituents of a flat universe. Shown are nonrelativistic matter, radiation, and a cosmological constant. All are in units of the critical density today. Even though matter and cosmological constant dominate today, at early times, the radiation density was largest. The epoch at which matter and radiation are equal is a_{eq} .

Dodelson,
Chapter 1

COSMIC BLACK-BODY RADIATION*

1965APJ...142...414D

One of the basic problems of cosmology is the singularity characteristic of the familiar cosmological solutions of Einstein's field equations. Also puzzling is the presence of matter in excess over antimatter in the universe, for baryons and leptons are thought to be conserved. Thus, in the framework of conventional theory we cannot understand the origin of matter or of the universe. We can distinguish three main attempts to deal with these problems.

1. The assumption of continuous creation (Bondi and Gold 1948; Hoyle 1948), which avoids the singularity by postulating a universe expanding for all time and a continuous but slow creation of new matter in the universe.
2. The assumption (Wheeler 1964) that the creation of new matter is intimately related to the existence of the singularity, and that the resolution of both paradoxes may be found in a proper quantum mechanical treatment of Einstein's field equations.
3. The assumption that the singularity results from a mathematical over-idealization,

* This research was supported in part by the National Science Foundation and the Office of Naval Research of the U.S. Navy.

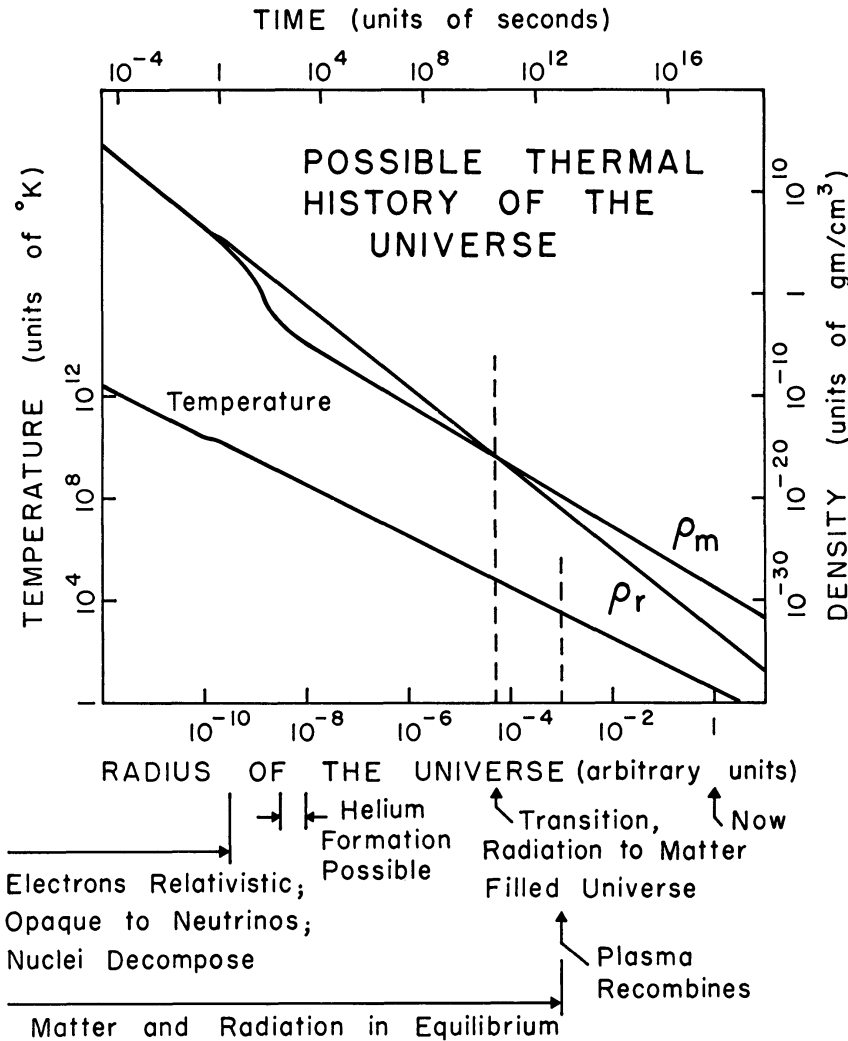


FIG 1 —Possible thermal history of the Universe. The figure shows the previous thermal history of the Universe assuming a homogeneous isotropic general-relativity cosmological model (no scalar field) with present matter density 2×10^{-29} gm/cm³ and present thermal radiation temperature 3.5° K. The bottom horizontal scale may be considered simply the proper distance between two chosen fiducial co-moving galaxies (points). The top horizontal scale is the proper world time. The line marked "temperature" refers to the temperature of the thermal radiation. Matter remains in thermal equilibrium with the radiation until the plasma recombines, at the time indicated. Thereafter further expansion cools matter not gravitationally bound faster than the radiation. The mass density in radiation is ρ_r . At present ρ_r is substantially below the mass density in matter, ρ_m , but, in the early Universe ρ_r exceeded ρ_m . We have indicated the time when the Universe exhibited a transition from the characteristics of a radiation-filled model to those of a matter-filled model.

Looking back in time, as the temperature approaches 10^{10} °K the electrons become relativistic, and thermal electron-pair creation sharply increases the matter density. At temperatures somewhat greater than 10^{10} °K these electrons should be so abundant as to assure a thermal neutrino abundance and a thermal neutron-proton abundance ratio. A temperature of this order would be required also to decompose the nuclei from the previous cycle in an oscillating Universe. Notice that the nucleons are non-relativistic here.

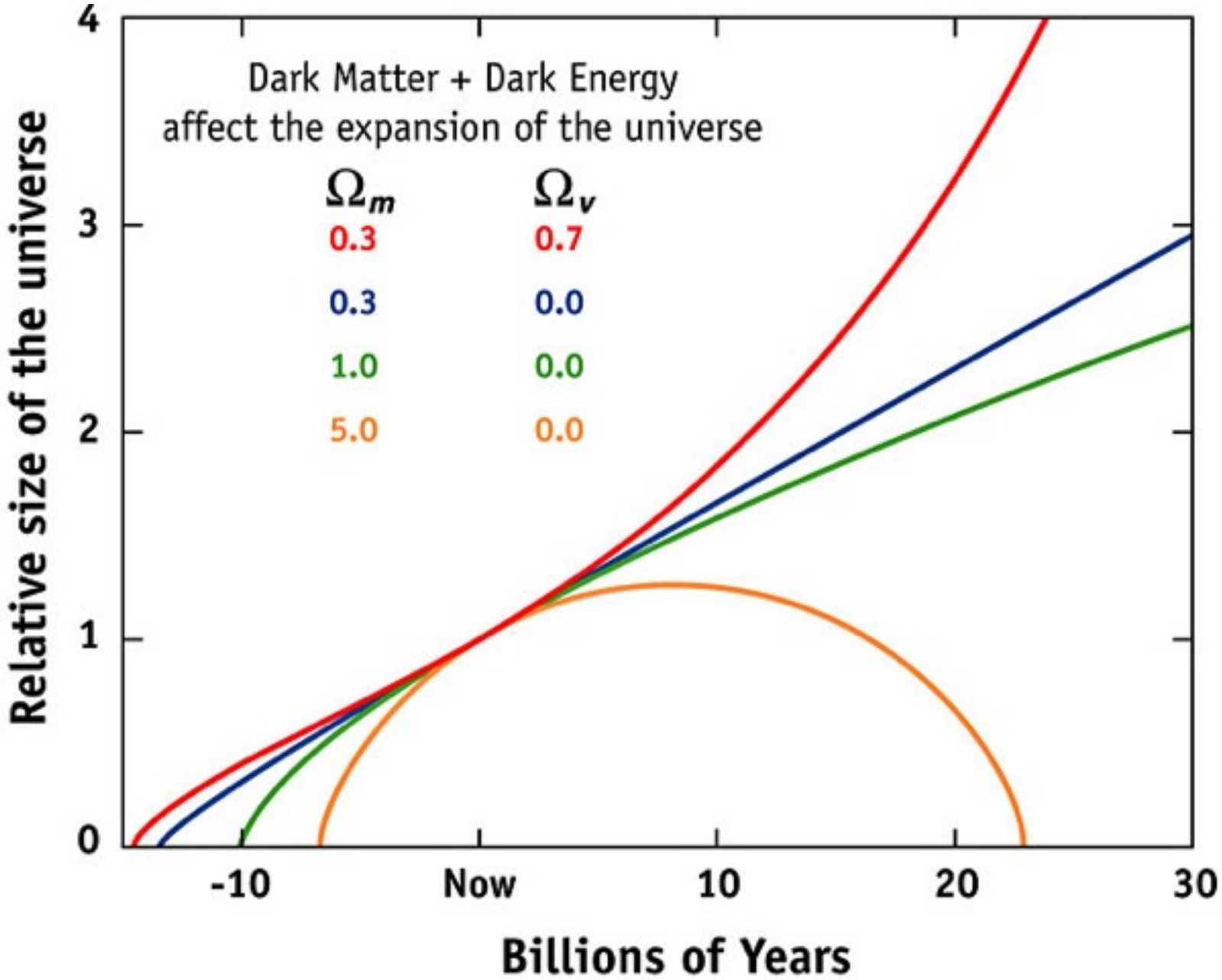
The thermal neutrons decay at the right-hand limit of the indicated region of helium formation. There is a left-hand limit on this region because at higher temperatures photodissociation removes the deuterium necessary to form helium. The difficulty with this model is that most of the matter would end up in helium.

We deeply appreciate the helpfulness of Drs. Penzias and Wilson of the Bell Telephone Laboratories, Crawford Hill, Holmdel, New Jersey, in discussing with us the result of their measurements and in showing us their receiving system. We are also grateful for several helpful suggestions of Professor J. A. Wheeler.

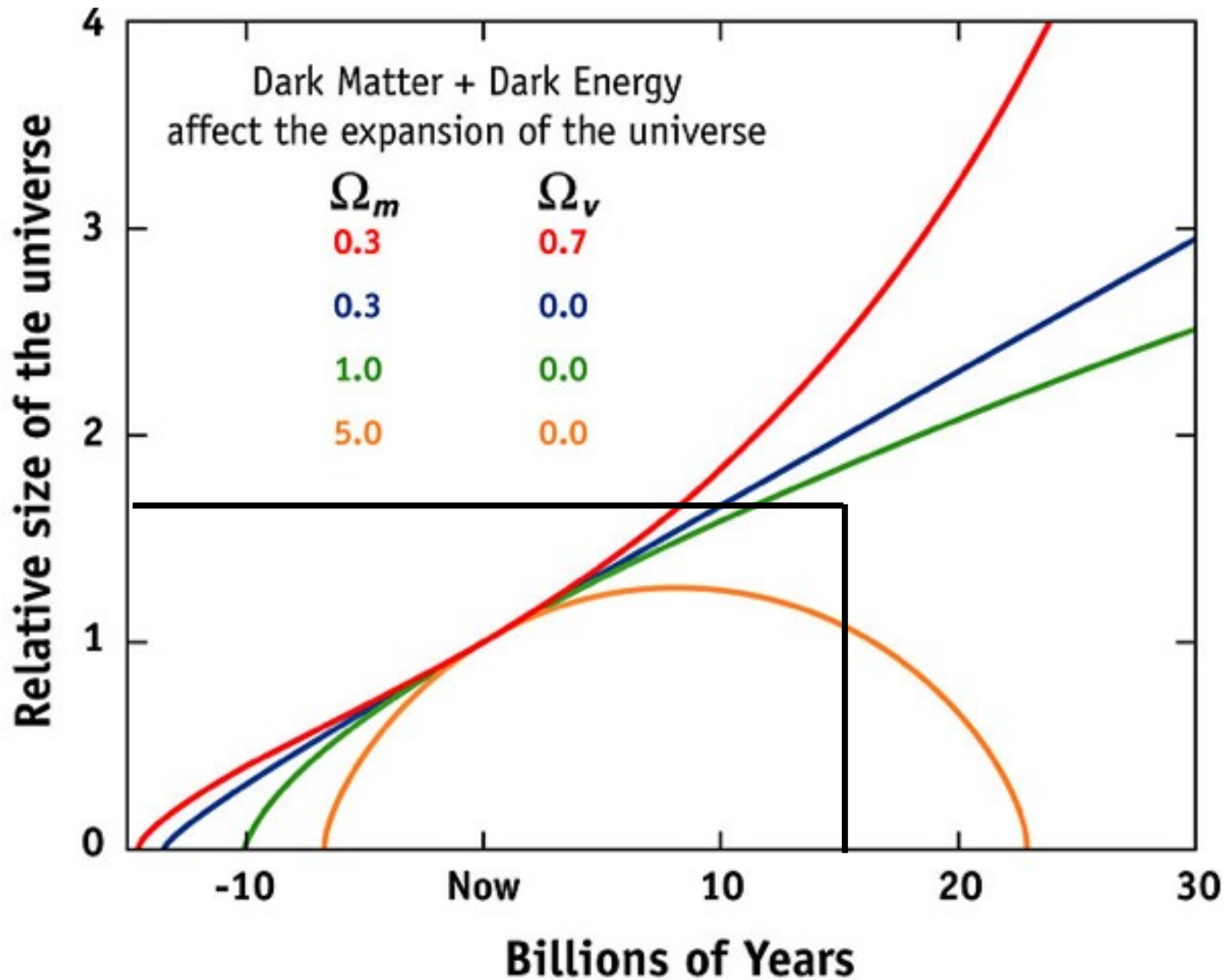
R. H. DICKE
P. J. E. PEEBLES
P. G. ROLL
D. T. WILKINSON

May 7, 1965
PALMER PHYSICAL LABORATORY
PRINCETON, NEW JERSEY

History of Cosmic Expansion for General Ω_M & Ω_Λ



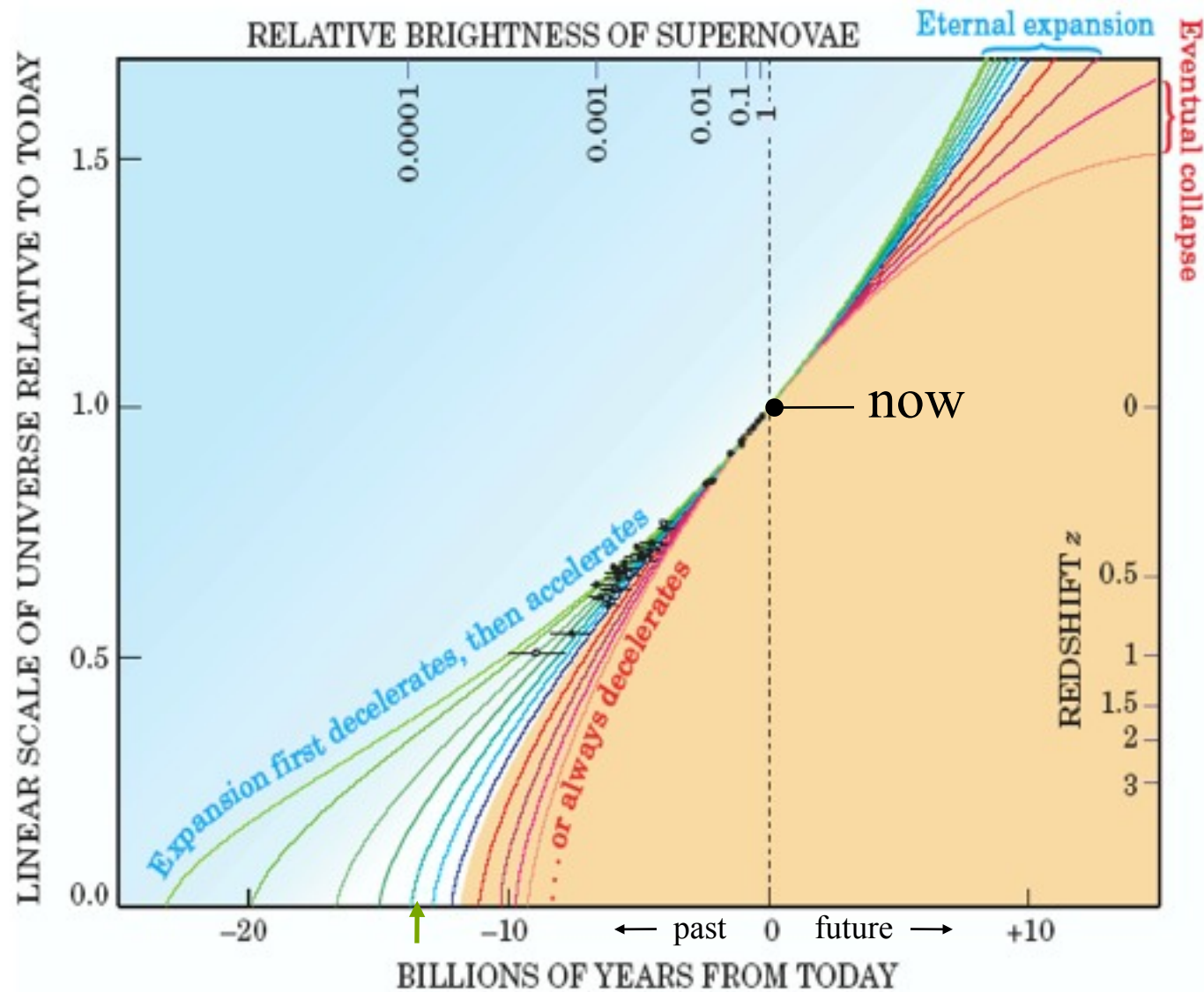
History of Cosmic Expansion for General Ω_M & Ω_Λ



History of Cosmic Expansion for $\Omega_\Lambda = 1 - \Omega_M$

With $\Omega_\Lambda = 0$ the age of the decelerating universe would be only 9 Gyr, but $\Omega_\Lambda = 0.7, \Omega_m = 0.3$ gives an age of 14 Gyr, consistent with stellar and radioactive decay ages

Figure 4. The history of cosmic expansion, as measured by the high-redshift supernovae (the black data points), assuming flat cosmic geometry. The scale factor R of the universe is taken to be 1 at present, so it equals $1/(1+z)$. The curves in the blue shaded region represent cosmological models in which the accelerating effect of vacuum energy eventually overcomes the decelerating effect of the mass density. These curves assume vacuum energy densities ranging from $0.95 \rho_c$ (top curve) down to $0.4 \rho_c$. In the yellow shaded region, the curves represent models in which the cosmic expansion is always decelerating due to high mass density. They assume mass densities ranging (left to right) from $0.8 \rho_c$ up to $1.4 \rho_c$. In fact, for the last two curves, the expansion eventually halts and reverses into a cosmic collapse.



ΛCDM Benchmark Cosmological Model: Ingredients & Epochs

	List of Ingredients
photons:	$\Omega_{\gamma,0} = 5.0 \times 10^{-5}$
neutrinos:	$\Omega_{\nu,0} = 3.4 \times 10^{-5}$
total radiation:	$\Omega_{r,0} = 8.4 \times 10^{-5}$
baryonic matter:	$\Omega_{\text{bary},0} = 0.04$
nonbaryonic dark matter:	$\Omega_{\text{dm},0} = 0.26$
total matter:	$\Omega_{m,0} = 0.30$
cosmological constant:	$\Omega_{\Lambda,0} \approx 0.70$

	Important Epochs	
radiation-matter equality:	$a_{rm} = 2.8 \times 10^{-4}$	$t_{rm} = 4.7 \times 10^4 \text{ yr}$
matter-lambda equality:	$a_{m\Lambda} = 0.75$	$t_{m\Lambda} = 9.8 \text{ Gyr}$
Now:	$a_0 = 1$	$t_0 = 13.5 \text{ Gyr}$

Benchmark Model: Scale Factor vs. Time

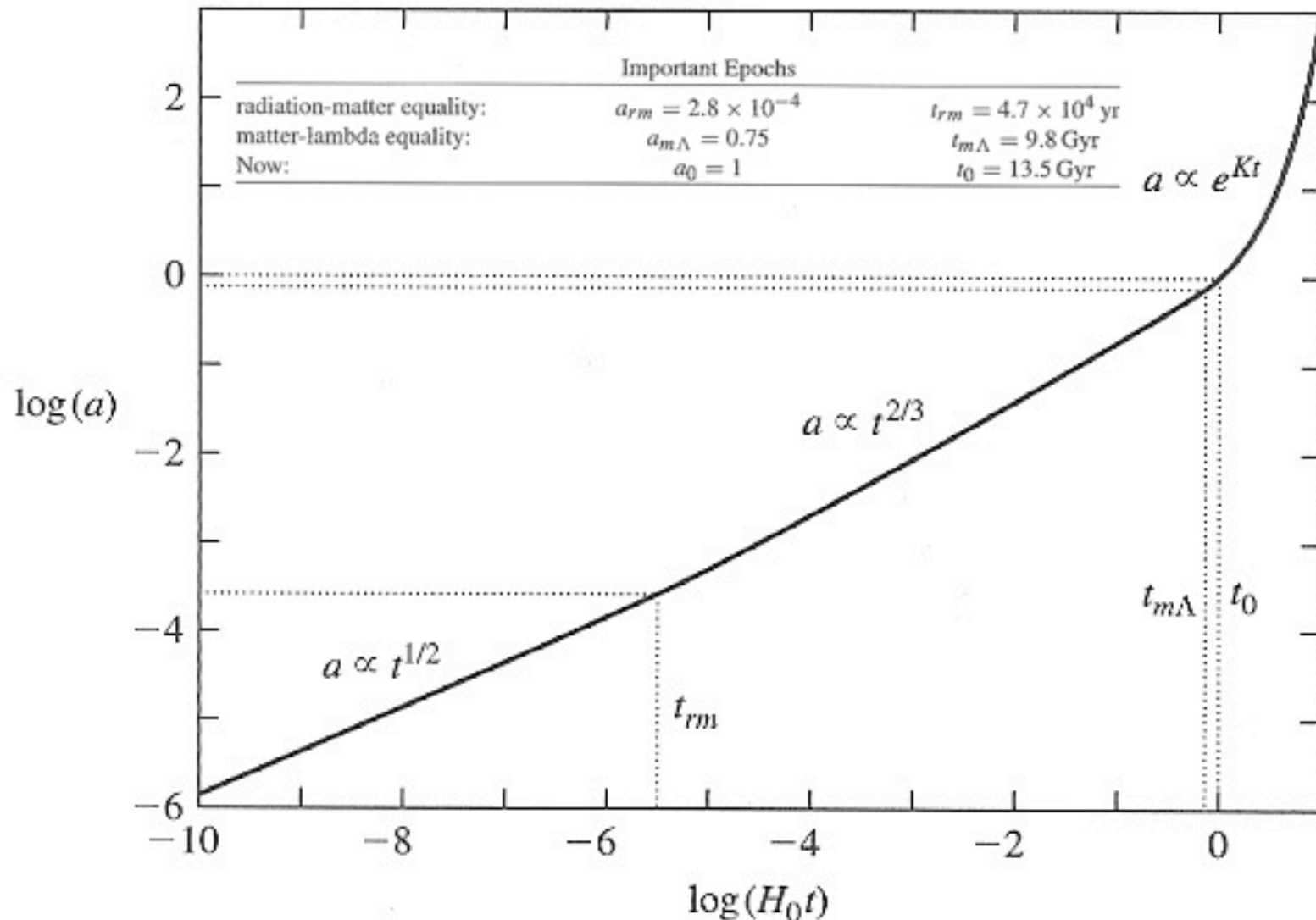
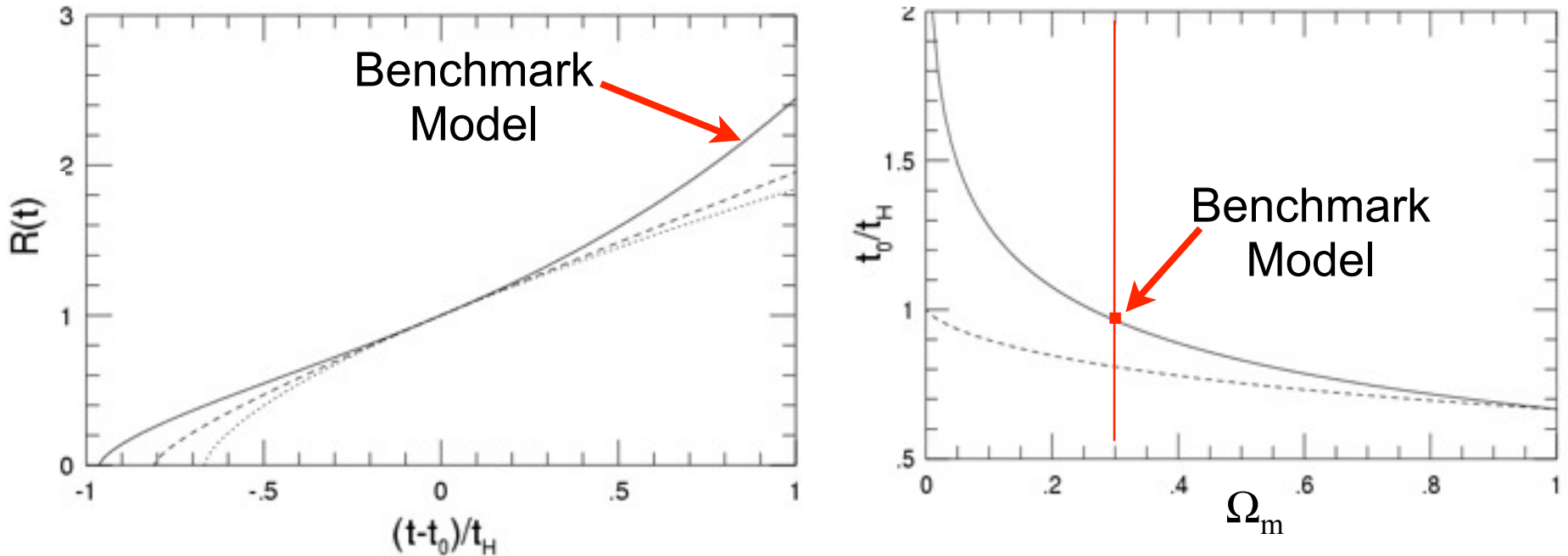


FIGURE 6.5 The scale factor a as a function of time t (measured in units of the Hubble time), computed for the Benchmark Model. The dotted lines indicate the time of radiation-matter equality, $a_{rm} = 2.8 \times 10^{-4}$, the time of matter-lambda equality, $a_{m\Lambda} = 0.75$, and the present moment, $a_0 = 1$.

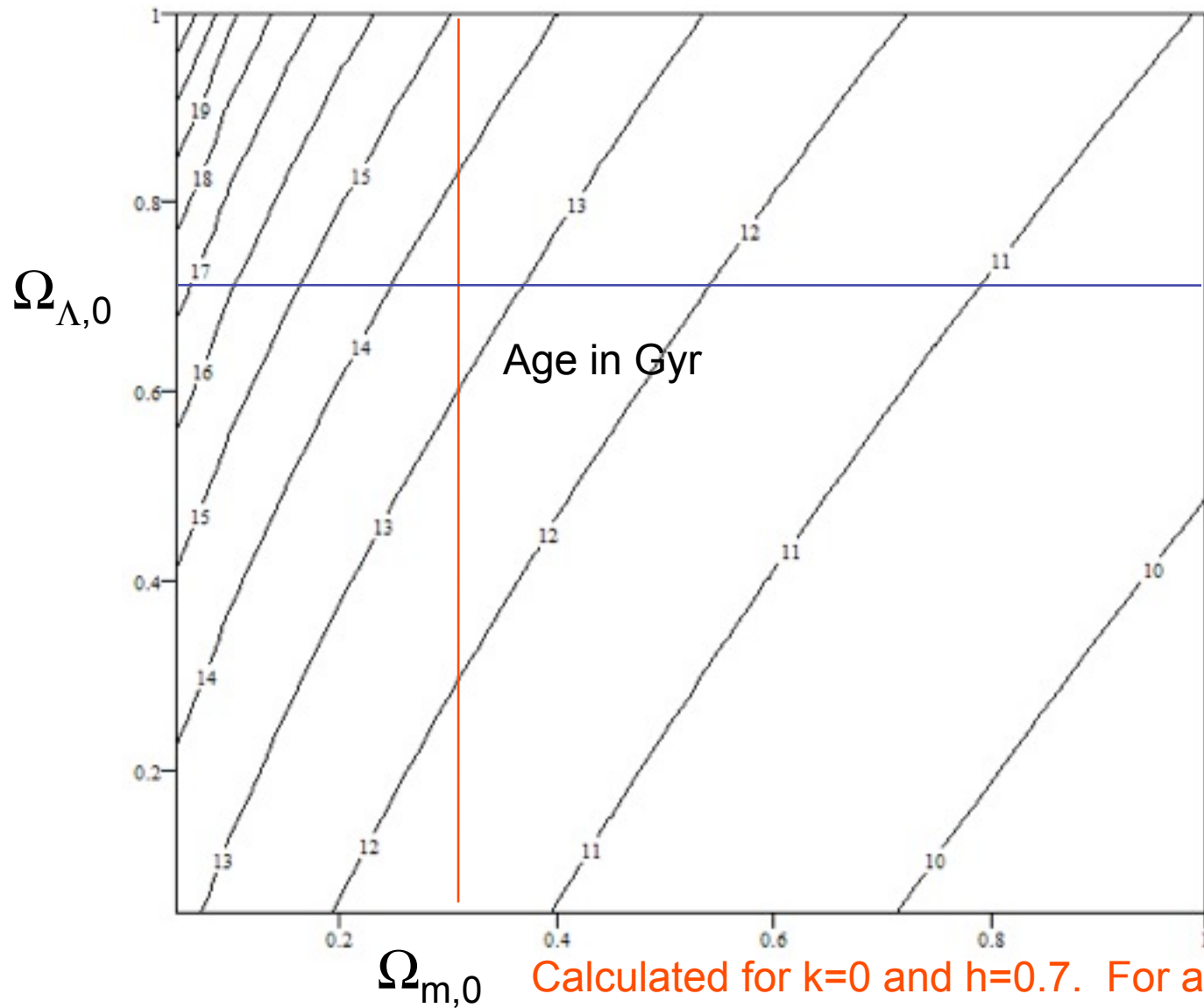
Barbara Ryden, *Introduction to Cosmology* (Addison-Wesley, 2003)

Age of the Universe t_0 in FRW Cosmologies



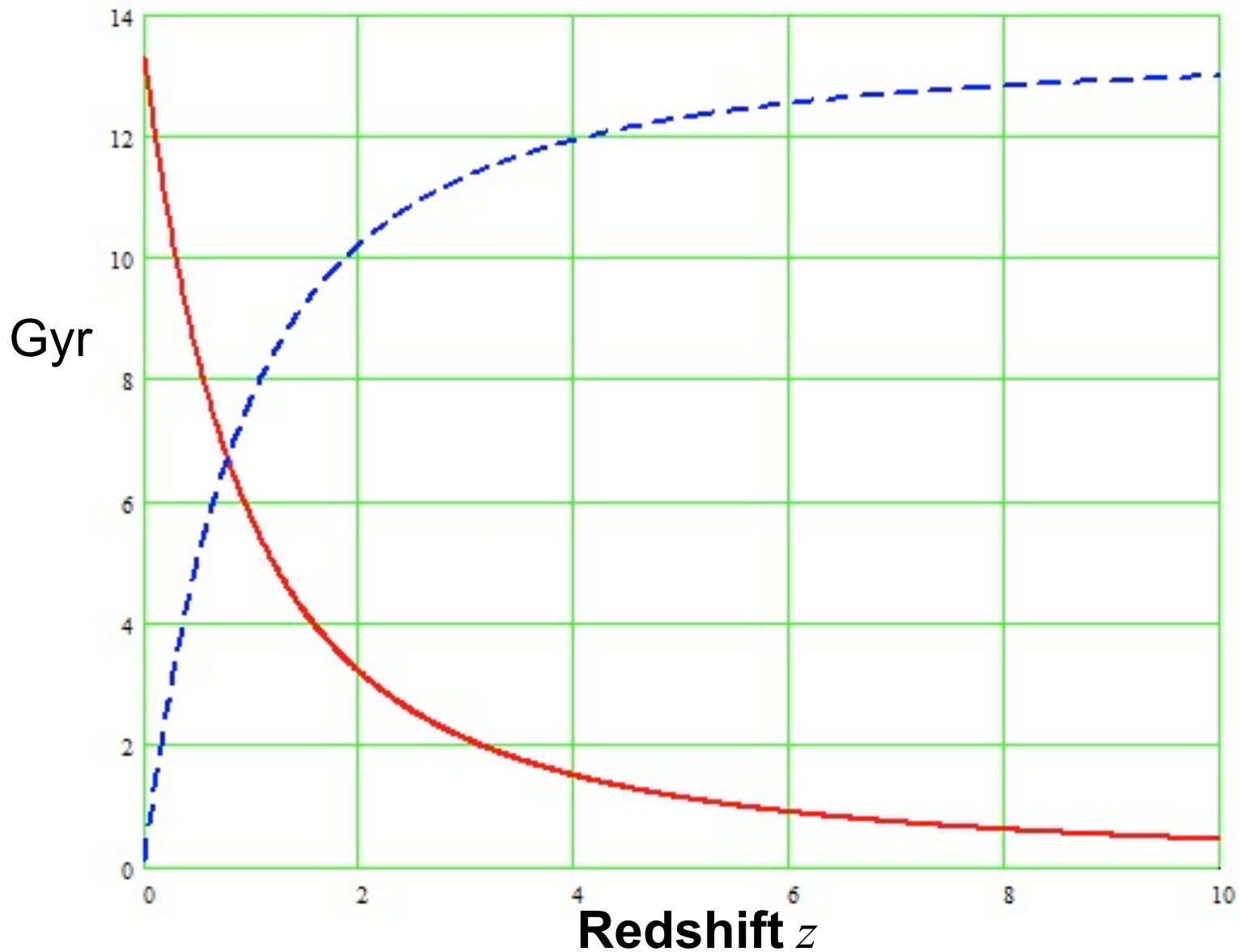
(a) Evolution of the scale factor $a(t)$ plotted vs. the time after the present $(t - t_0)$ in units of Hubble time $t_H \equiv H_0^{-1} = 9.78h^{-1}$ Gyr for three different cosmologies: Einstein-de Sitter ($\Omega_0 = 1, \Omega_\Lambda = 0$ dotted curve), negative curvature ($\Omega_0 = 0.3, \Omega_\Lambda = 0$: dashed curve), and low- Ω_0 flat ($\Omega_0 = 0.3, \Omega_\Lambda = 0.7$: solid curve). (b) Age of the universe today t_0 in units of Hubble time t_H as a function of Ω_0 for $\Lambda = 0$ (dashed curve) and flat $\Omega_0 + \Omega_\Lambda = 1$ (solid curve) cosmologies.

Age t_0 of the Double Dark Universe

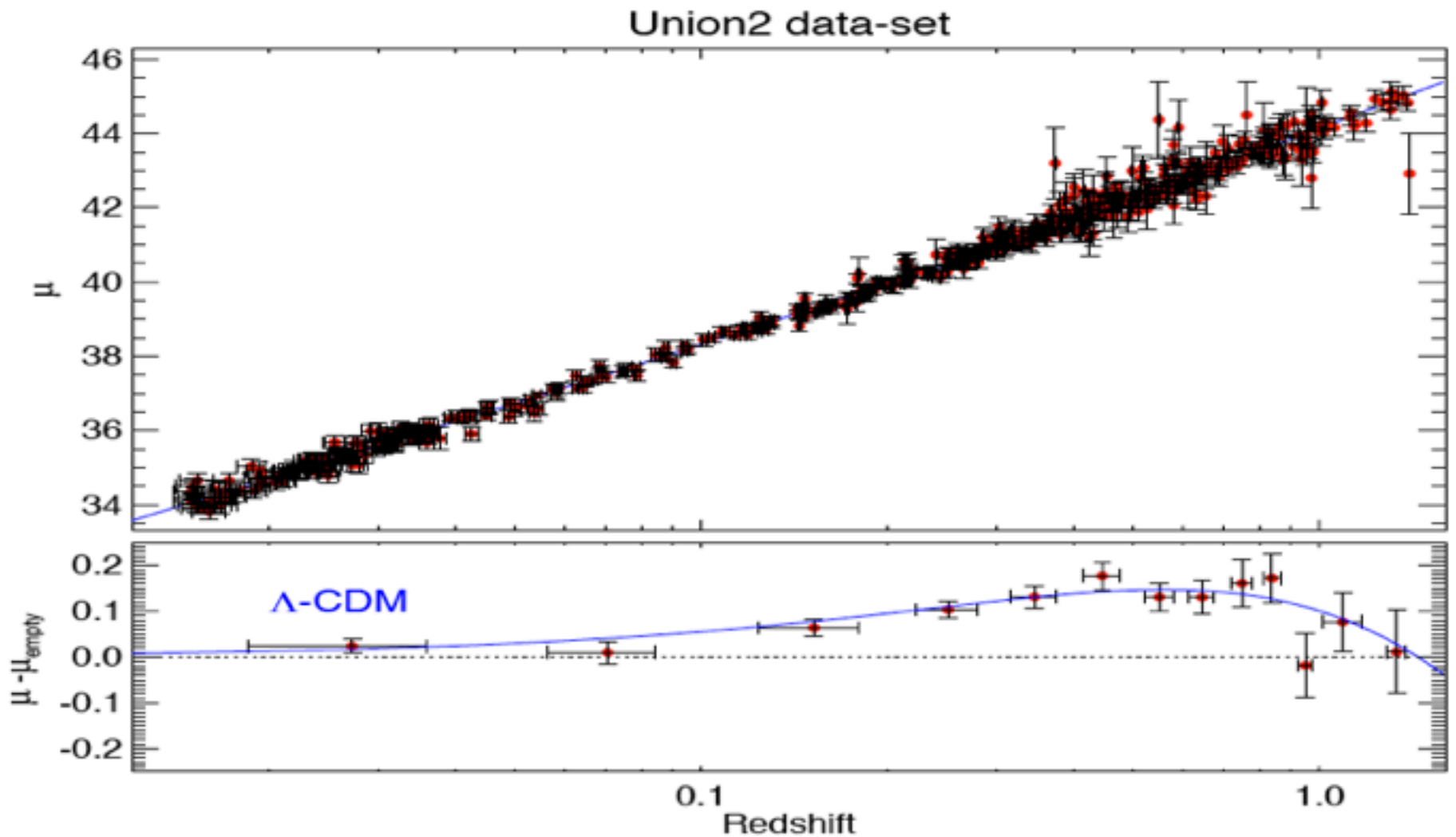


Calculated for $k=0$ and $h=0.7$. For any other value of the Hubble parameter, multiply the age by $(h/0.7)$.

Age of the Universe and Lookback Time



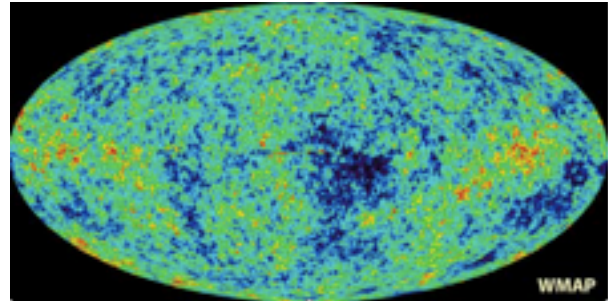
These are for the **Benchmark Model** $\Omega_{m,0}=0.3$, $\Omega_{\Lambda,0}=0.7$, $h=0.7$.



The Hubble diagram of Type Ia supernovae correlating distance modulus (μ) vs. redshift. The Union2 compilation (Amanullah R, Lidman C, Rubin D, Aldering G, Astier P, et al., 2010) represents the currently largest SN Ia sample. The linear expansion in the local universe can be traced out to $z < 0.1$. The distance relative to an empty universe model (μ_{empty}) is shown in the lower panel. The data are binned for clarity in this diagram. The blue curve shows the expectation from the best fit Λ CDM model with $\Omega_m = 0.3$.

Brief History of the Universe

- Cosmic Inflation generates density fluctuations
- Symmetry breaking: more matter than antimatter
- All antimatter annihilates with almost all the matter (1s)
- Big Bang Nucleosynthesis makes light nuclei (10 min)
- Electrons and light nuclei combine to form atoms, and the cosmic background radiation fills the newly transparent universe (380,000 yr)
- Galaxies and larger structures form (~ 1 Gyr)
- Carbon, oxygen, iron, ... are made in stars
- Earth-like planets form around 2nd generation stars
- Life somehow starts (~ 4 Gyr ago) and evolves on earth

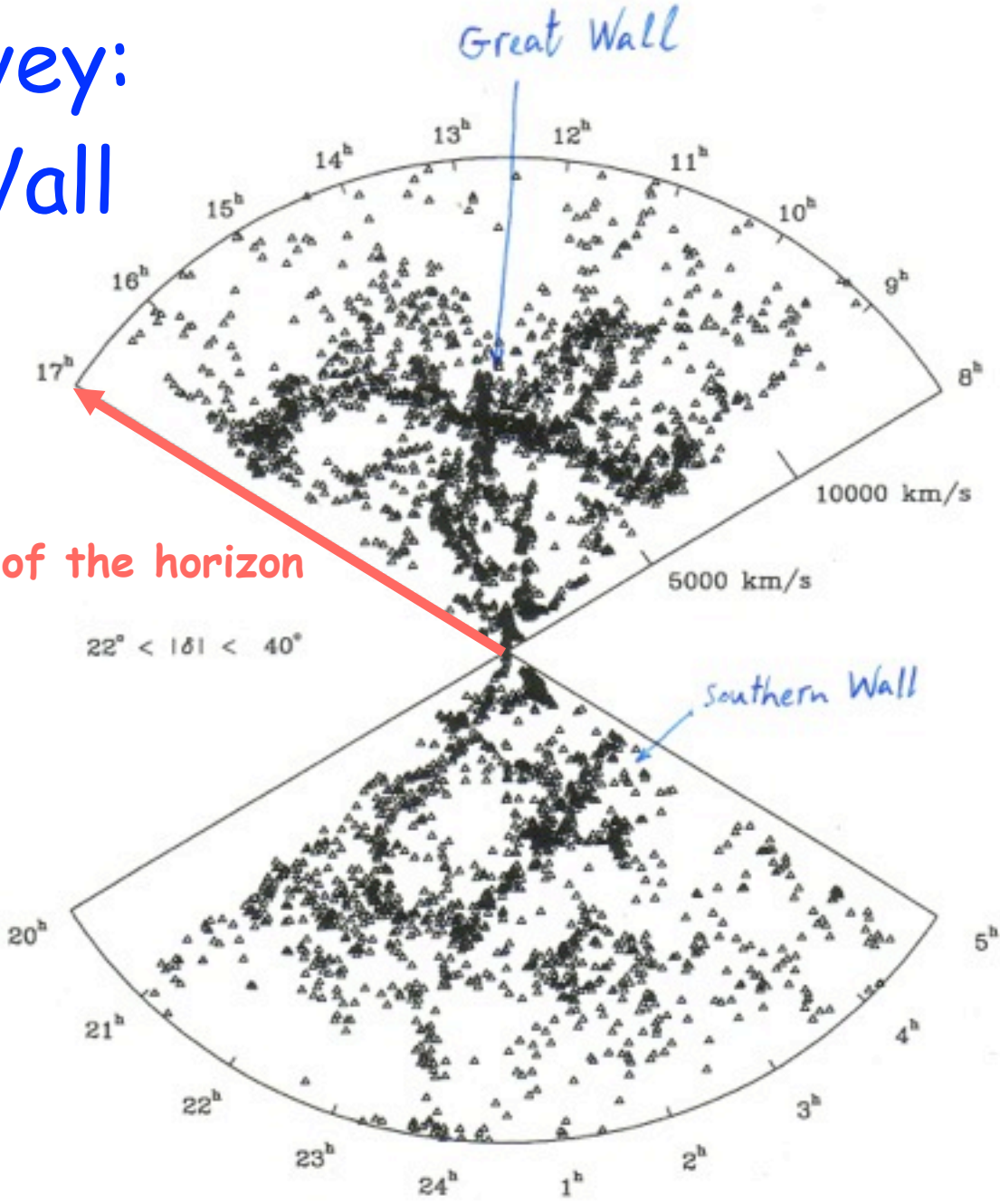


Mapping the large scale structure of the universe ...

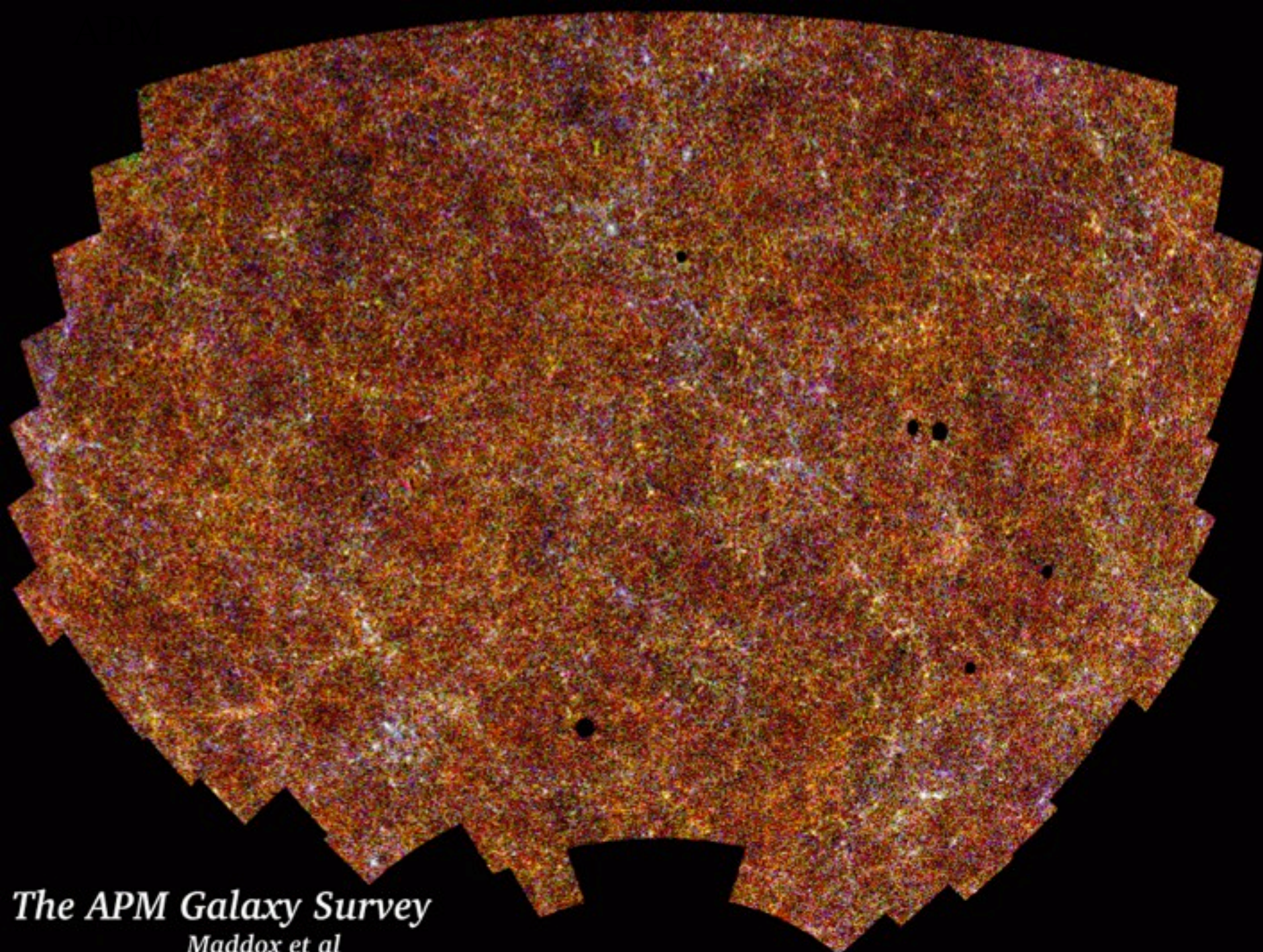
Lick Survey
1M galaxies

North Galactic

CfA survey: Great Wall



1/20 of the horizon



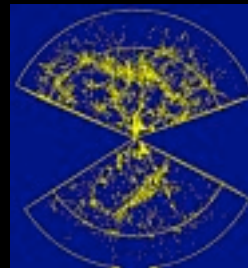
The APM Galaxy Survey
Maddox et al

2dF Galaxy Redshift Survey

$\frac{1}{4}$ M galaxies 2003

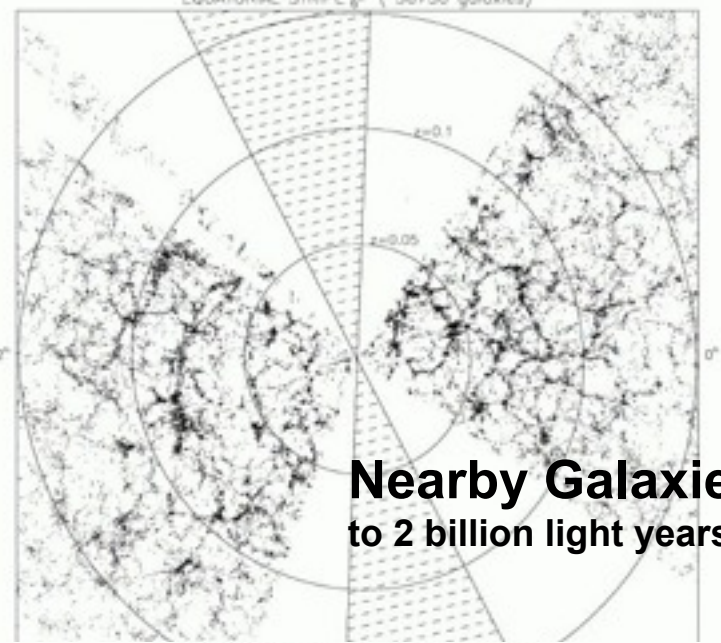
1/4 of the horizon

CFA Survey
1983

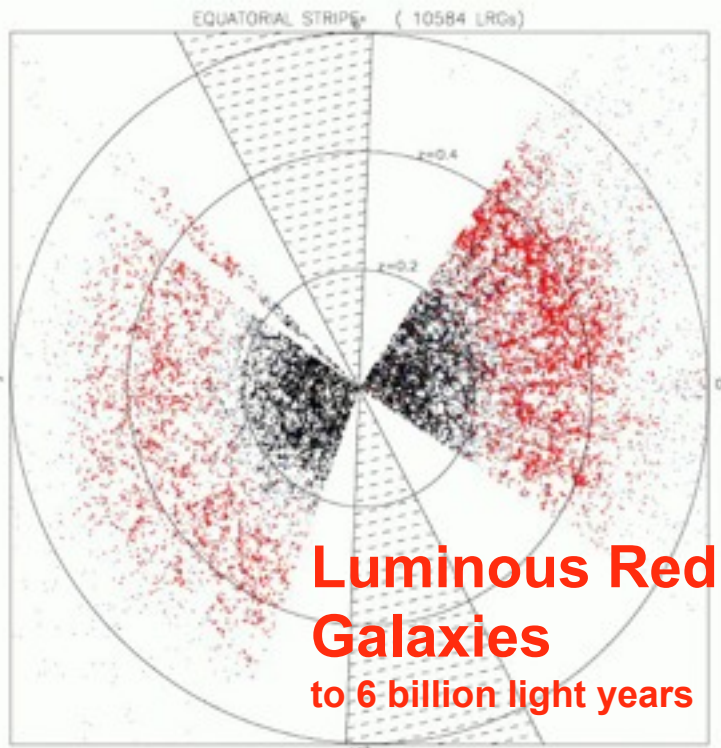


Mapping the Galaxies Sloan Digital Sky Survey

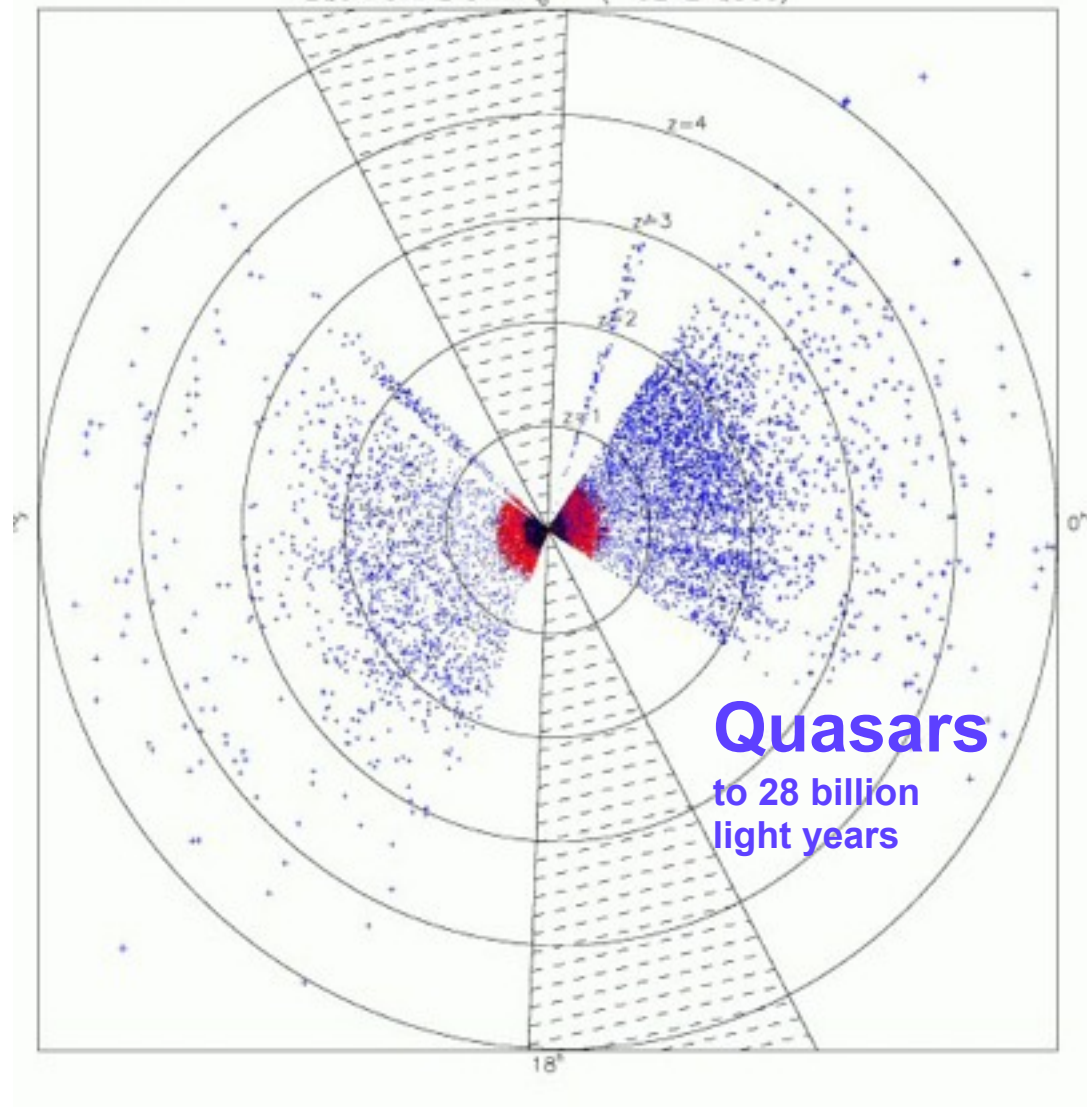
Nearby Galaxies
to 2 billion light years



Luminous Red Galaxies
to 6 billion light years



EQUATORIAL STRIPE⁺ (9242 QSOs)



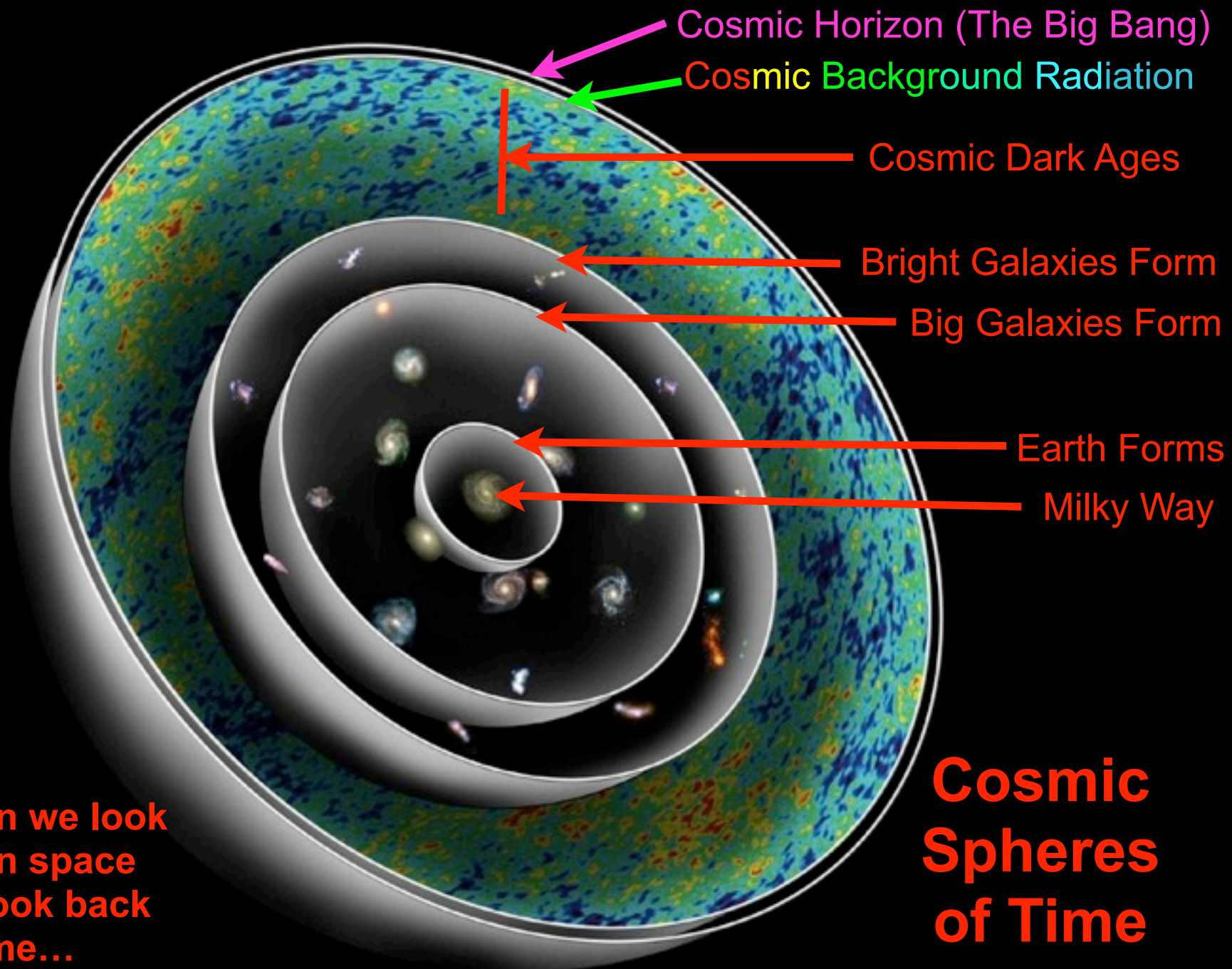
Quasars
to 28 billion
light years

GALAXIES MAPPED BY THE SLOAN SURVEY

Data Release 4:

565,715 Galaxies & 76,403 Quasars

GALAXIES MAPPED BY THE SLOAN SURVEY



Cosmic Horizon (The Big Bang)

Cosmic Background Radiation

Cosmic Dark Ages

Bright Galaxies Form

Big Galaxies Form

Earth Forms

Milky Way

When we look out in space we look back in time...

Cosmic Spheres of Time

Medieval Universe



The geocentric pre-Copernican Universe in Christian Europe. At center, Earth is divided into Heaven (tan) and Hell (brown). The elements water (green), air (blue) and fire (red) surround the Earth. Moving outward, concentrically, are the spheres containing the seven planets, the Moon and the Sun, as well as the "Twelve Orders of the Blessed Spirits," the Cherubim and the Seraphim. German manuscript, c. 1450.